Density Functional Theory-Based Nanostructure Investigation: Theoretical Considerations

D. Negrut* M. Anitescu† T. Munson‡ P. Zapol§

May 17, 2005

Abstract

This work proposes a theoretical framework for the investigation of chemical and mechanical properties of nanostructures. The methodology is based on a two-step approach to compute the electronic density distribution in and around a nanostructure, and then the displacement of its nuclei. The *Electronic Problem* embeds interpolation and coupled cross-domain optimization techniques through a process called electronic reconstruction. In the second stage of the solution, the *Ionic Problem* deals with repositioning the nuclei of the nanostructure given the electronic density in the domain. It is shown that the new ionic configuration is the solution of a non-linear system obtained based on a first order optimality condition when minimizing the total energy associated with the nanostructure. The long-term goal of this work is a substantial increase in the dimension of the nanostructures that can be simulated using approaches that include accurate DFT computation. The increase in nanostructure size results from the key observation that during the solution of the *Electronic Problem* expensive DFT calculations typically carried out with dedicated third party software such as NWChem or Gaussian03, are limited to a small number of subdomains; the electronic density is then reconstructed elsewhere. For the *Ionic Problem*, computational gains result from approximating the dislocation of the nuclei in terms of a reduced number of representative nuclei following the quasicontinuum paradigm.

1 Introduction

The intent of this document is to provide the analytical framework for a longer-term project that focuses on the investigation of chemical and mechanical properties of nanostructures.

Nanostructures have dimensions in the range of $1 \sim 100$ nm and typically contain $10^2 \sim 10^8$ atoms. Applying the well-established Kohn-Sham DFT method [18] for nonperiodic structures of 60 atoms has led to simulations that can take up to three months to complete. When long range interactions are ignored and pseudo-potentials are used, *ab-initio* simulations have been carried out for nonmetallic structures with up to 1,500 atoms [25]. The approach that enabled the increase in the number of atoms belongs to the family of so-called $\mathcal{O}(N)$ methods [10], which scale as N with the dimension of the problem (in this case the number of electrons).

This work is concerned with fundamental electronic structure computation methods. Acknowledging the small-dimension constraint placed on the problem by the existing Density Functional Theory (DFT)-based methods, the goal of the proposed work is to use techniques that, by closing the spatial scale gap, render electronic structure information at the nanoscale. This electronic structure information is then used to investigate the chemical and mechanical properties of the material.

In the context of mechanical analysis of nanostructures, the methodology proposed follows in the steps of the quasi-continuum work proposed in [26, 16, 7]. Specifically, this is an extension of the work in [26, 16], because rather than considering a potential-based interatomic interaction that has a limited range of validity and is difficult to generalize to inhomogeneous materials, the methodology proposed uses *ab-initio* methods to provide for the particle interaction. At the same time it is a generalization of the method proposed in [7] because rather than considering each mesh discretization element to be part of a periodic and uniformly deformed infinite crystal, the proposed method treats in a generic optimization framework any structure (nonperiodic and inhomogeneous) once the electronic density distribution is available.

Two goals are associated with this project; (1) development and software implementation of a methodology that can substantially increase the dimension attribute of the electronic structure problem, and (2) support

*Math. and Comp. Science Division, Argonne National Laboratory, Argonne, IL, USA. negrut@mcs.anl.gov
†Math. and Comp. Science Division, Argonne National Laboratory, Argonne, IL, USA. anitescu@mcs.anl.gov
‡Math. and Comp. Science Division, Argonne National Laboratory, Argonne, IL, USA. tmunson@mcs.anl.gov
§Chemistry and Materials Science Divisions, Argonne National Laboratory, Argonne, IL, USA. zapol@anl.gov

for investigation of general nanostructures (metallic and nonmetallic, nonperiodic structures, inhomogeneous materials).

1.1 Paradigm of the proposed approach

The electronic density reconstruction described is done in reference to a regular lattice or domain of a regular lattice. Significant computational savings are anticipated to stem from two assumptions: (1) the *geometric assumption*, where the premise is that the lattice is only minimally deformed and the state variables are nearly periodic in most of the domain (this latter requirement will be relaxed to allow for localized defects), and (2) the *electronic assumption*, where the premise is that for a given ionic distribution, the electronic energy can be expressed as

$$E(\rho, \rho_A) = \int \theta^1(\rho, \rho_A, \mathbf{r})\mathrm{d}\mathbf{r} + \iint \theta^2(\rho, \rho_A, \mathbf{r}; \rho, \rho_A, \mathbf{r}')\mathrm{d}\mathbf{r}\mathrm{d}\mathbf{r}' \tag{1}$$

This representation is commonly used in conjunction with the so-called Orbital-Free DFT (OFDFT) method [29]. Here $\theta^{1,2}$ are the relevant energy density functions; ρ is the electronic density; and ρ_A is the nuclear density, which may include delta functions. The first term typically includes the kinetic energy and an exchange-correlation term, whereas the second integral includes all pairwise interactions. Details regarding the definition of these terms are provided by several authors [20, 15, 17].

The electronic structure computation is then formulated as an optimization problem [14]: find the electronic density ρ that solves the problem

$$\min_{\rho} E[\rho, \rho_A] \tag{2a}$$

subject to the charge conservation constraint

$$\int \rho(\mathbf{r})\mathrm{d}\mathbf{r} = N_e \tag{2b}$$

where N_e represents the number of electrons present. The solution to this problem depends parametrically on the nuclear density ρ_A, $\rho = \rho(\rho_A)$, a consequence of the Born-Oppenheimer assumption. Subsequently, the computation of the ground state of the entire system as the solution of the optimization problem

$$\min_{\rho_A} E[\rho(\rho_A), \rho_A] \tag{3}$$

provides the nuclei distribution. The latter problem governs the approach to the first question.

As indicated above, one of the two *central assumptions* is that almost everywhere in the nanostructure the solution to the nuclei distribution problem results in only small deformations. In order to quantify the concept of small deformation, the nanostructure is considered to occupy an initial reference configuration $D^0 \subset \mathbb{R}^3$. The structure undergoes a change of shape described by a deformation mapping $\mathbf{\Phi}(\mathbf{r}^0, t) \in \mathbb{R}^3$. This deformation mapping gives the location $\mathbf{r}$ in the global Cartesian reference frame of each point $\mathbf{r}^0$ represented in the undeformed material frame. As indicated, the mapping might depend on time t. The variable t does not necessarily represent the time contemporary with the structure under consideration. In fact, in a quasi-state simulation framework, this variable might be an iteration index of an optimization algorithm that solves Eq.(3) in the case ρ_A is made of nuclear point charges.

The components of the deformation gradient are introduced as

$$F_{iJ} = \frac{\partial \Phi_i}{\partial r^0_J} \tag{4}$$

where upper-case indices refer to the material frame, and lower-case indices to the Cartesian global frame. Thus, $\mathbf{F} = \nabla_0 \mathbf{\Phi}$, where ∇_0 represents the material gradient operator, and therefore the deformation of an infinitesimal material neighborhood $\mathrm{d}\mathbf{r}^0$ about a point $\mathbf{r}^0$ of D^0 is expressed as

$$\mathrm{d}r_i = F_{iJ}\ \mathrm{d}r^0_J \tag{5}$$

The concept of small distortion is equivalent to requiring that the spectral radius of $\mathbf{F}$ be sufficiently small; that is,

$$||\nabla_0\ \mathbf{\Phi}||_2 < \mathcal{K} \tag{6}$$

is expected to hold for almost everywhere in the domain $\mathbf{B}_0$, for a suitable chosen value of $\mathcal{K}$.

As a consequence of the *geometric assumption*, computational savings are anticipated because for all the domains that satisfy the condition of Eq.(6) a two-tier interpolation-based approach will reduce the dimension of

the problem. First, the electronic structure will be reconstructed in some domains by interpolation using adjacent regions in which a DFT-based approach has been used to accurately solve the electronic structure problem; we call this procedure *electronic density reconstruction*. Second, the position of the nuclei will be expressed in terms of the positions of a reduced set of so-called representative nuclei, *repnuclei*, in an approach similar to the one proposed in [26]. The proposed approach solves only for the position of these *repnuclei*; the position of the rest of the nuclei is then obtained by interpolation.

The remainder of this document is organized as follows. Section 2 discusses the strategy for electronic density reconstruction. The emphasis is placed on how interpolation is used to estimate the value of the electronic density in an entire domain D based on information available in a limited set of interior subdomains. The section starts with a simple DFT approach (Thomas-Fermi) that serves as a vehicle for introducing of an otherwise abstract methodology. The entire section draws on the physics of the problem being addressed. In contrast, section 3 focuses on the numerical solution component of the methodology. This section casts the problem in a numerical optimization framework and then presents the difficulties associated with the problem and the way they are addressed. With the electronic structure problem solved, the proposed methodology uses the Born-Oppenheimer assumption to investigate the mechanical properties of a nanostructure given a certain electronic distribution. This analysis is discussed in section 4. Section 5 succinctly presents an outline of the computational flow at the end of which the coupled electronic structure and nanostructure shape problems are solved together. A set of open questions conclude this section. Following the Conclusions section, the Appendix presents a more formal proof for a domain decomposition approach used within the Thomas-Fermi DFT framework.

2 Electronic Density Reconstruction

2.1 A simple example: a domain with a gap and Thomas-Fermi DFT

The notation introduced in section 1.1 as well as the proposed methodology is first applied when the Thomas-Fermi functional is used to describe the dependency of the energy on electronic density [27, 8]. The Thomas-Fermi functional has well-known severe accuracy limitations. It provides, however, a simple framework in which several key points of the methodology proposed for electronic density reconstruction are more easily introduced.

2.1.1 The Thomas-Fermi functional

The Thomas-Fermi-based energy functional assumes the form

$$E\left[\rho, \{\mathbf{R}_A\}\right] = E_{ne}\left[\rho, \{\mathbf{R}_A\}\right] + J\left[\rho\right] + K\left[\rho\right] + T\left[\rho\right] + V_{nn}\left(\{\mathbf{R}_A\}\right) \tag{7}$$

where

$$E_{ne}\left[\rho, \{\mathbf{R}_A\}\right] = -\sum_{A=1}^{M} \int \frac{Z_A\, \rho(\mathbf{r})}{\|\mathbf{R}_A - \mathbf{r}\|}\, \mathrm{d}\mathbf{r} \tag{8a}$$

$$J\left[\rho\right] = \frac{1}{2} \int \int \frac{\rho(\mathbf{r})\, \rho(\mathbf{r}')}{\|\mathbf{r} - \mathbf{r}'\|}\, \mathrm{d}\mathbf{r}\, \mathrm{d}\mathbf{r}' \tag{8b}$$

$$T\left[\rho\right] = C_F \int \rho^{\frac{5}{3}}(\mathbf{r})\, \mathrm{d}\mathbf{r} \tag{8c}$$

$$K\left[\rho\right] = -C_x \int \rho^{\frac{4}{3}}(\mathbf{r})\, \mathrm{d}\mathbf{r} \tag{8d}$$

$$V_{nn}\left(\{\mathbf{R}_A\}\right) = \sum_{A=1}^{M} \sum_{B=A+1}^{M} \frac{Z_A\, Z_B}{\|\mathbf{R}_A - \mathbf{R}_B\|} \tag{8e}$$

Here $C_F = \frac{3}{10}(3\pi^2)^{2/3}$, and $C_x = \frac{3}{4}\left(\frac{3}{\pi}\right)^{1/3}$, and the following notation is used:

- E_{ne} - energy corresponding to nucleus-electron interaction
- J - Coulomb energy
- K - exchange energy
- T - kinetic energy
- V_{nn} - inter-nuclear interaction energy
- Z_A - atomic number associated with nucleus A

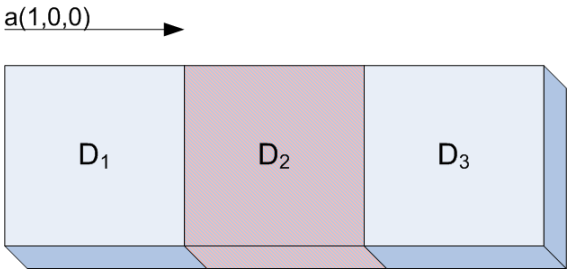

Figure 1: Electronic density reconstruction.

- $\mathbf{r}_i$ - global position of electron i
- $\mathbf{R}_A$ - global position of nucleus of atom A
- $\int(\cdot)$ without integration limits - an integral over the entire domain.

The expression of the energy functional of Eq.(7) justifies the notation used in Eq.(1): the kinetic, exchange, and nuclear electronic energy are represented through the θ^1 term; the electron-electron interaction is associated with the term θ^2.

In this simple example assume that there are three identical domains D_1, D_2, D_3, as in Fig.1. The electronic density in the respective domains is denoted by $\rho_1(\mathbf{r}), \rho_2(\mathbf{r}), \rho_3(\mathbf{r})$:

$$\rho(\mathbf{r}) = \begin{cases} \rho_1(\mathbf{r}) & \mathbf{r} \in D_1 \\ \rho_2(\mathbf{r}) & \mathbf{r} \in D_2 \\ \rho_3(\mathbf{r}) & \mathbf{r} \in D_3 \end{cases}$$

The definition of the density outside the domain $D_1 \cup D_2 \cup D_3$ is extended by assuming that its value is zero.

In the Thomas-Fermi case, the optimization problem of Eq.(2) depends parametrically on the positions of the nuclei:

$$\begin{array}{ll} \min_\rho & E(\rho; \{\mathbf{R}_A\}) + \lambda \left(\int \rho dr - N \right) \\ s.t. & \int \rho dr - N = 0 \end{array} \tag{9}$$

The constrained optimization problem above is formulated for the case in which there is no deformation in the underlying crystal structure of the material, whose nuclei are at positions $\{\mathbf{R}_A\}$, for $A = 1 \dots M$. In a direct approach, the dimension of the problem is prohibitive most of the time; unless simplifying assumptions are taken into account (such as periodic boundary conditions, local effects (truncation), pseudo-potentials, etc.), systems that contain thousands of atoms cannot be typically simulated. For domains $D_i, i = 1, 2, 3$, the energy is defined as

$$\begin{aligned} E_i\left[\rho_i, \lambda_i; \bar{\rho}_i, \{R_A\}\right] &= C_F \int_{D_i} \rho_i^{\frac{5}{3}}(\mathbf{r})\, d\mathbf{r} - C_x \int_{D_i} \rho_i^{\frac{4}{3}}(\mathbf{r})\, d\mathbf{r} + \int_{D_i} \int_{D-D_i} \frac{\rho_i(\mathbf{r})\, \bar{\rho}_i(\mathbf{r}')}{\|\mathbf{r} - \mathbf{r}'\|}\, d\mathbf{r}\, d\mathbf{r}' \\ &+ \frac{1}{2} \int_{D_i} \int_{D_i} \frac{\rho_i(\mathbf{r})\, \bar{\rho}_i(\mathbf{r}')}{\|\mathbf{r} - \mathbf{r}'\|}\, d\mathbf{r}\, d\mathbf{r}' - \sum_{A=1}^{M} \int_{D_i} \frac{Z_A\, \rho_i(\mathbf{r})}{\|\mathbf{R}_A - \mathbf{r}\|}\, d\mathbf{r} + \lambda_i \int_{D_i} \rho_i\, d\mathbf{r} \end{aligned} \tag{10}$$

We use the symbol $\bar{\rho}_i$ to denote the electronic density outside the domain D_i, $i = 1, 2, 3$. The optimality conditions for the optimization problem (9) can now be represented in terms of subdomain problems on the domains D_i, $i = 1, 2, 3$.

$$\nabla_{\rho_i} E_i(\rho_i, \lambda_i; \bar{\rho}_i, \{\mathbf{R}_A\}) = 0, \quad i = 1, 2, 3 \tag{11a}$$

$$\lambda_1 = \lambda_2 = \lambda_3 \tag{11b}$$

$$\int \rho \mathrm{d}\mathbf{r} - N_e = 0 \tag{11c}$$

2.1.2 Reconstruction through interpolation

Assuming that the solution is sufficiently close to, but not necessarily, periodic, for $\mathbf{r} \in D_2$ the density is reconstructed by averaging, that is (see Fig.1)

$$\rho_2(\mathbf{r}) \approx \frac{1}{2}\left(\rho_1(\mathbf{r} - a(1,0,0)) + \rho_3(\mathbf{r} + a(1,0,0))\right) \tag{12}$$

where $a(1,0,0)$ is a translation vector that indicates that the structure is periodic in the $(1,0,0)$ direction. Likewise, $a > 0$ is a constant scaling factor associated with the underlying structure, much as it is the case with a Bravais lattice but in this case applied for subdomain-type periodicity.
This approximation can be improved by using only domains away from the endpoints of the overall slab-like domain. However, for simplicity, in this example the entire domains D_1 and D_3 are considered for reconstruction. Based on Eqs.(11) and (12), this leads to the following coupled system of nonlinear equations

$$\nabla_{\rho_1} E_1(\rho_1, \lambda_1; \rho_3, \frac{1}{2}\left(\rho_1(r - a(1,0,0)) + \rho_3(r + a(1,0,0))\right), \{\mathbf{R}_A\}) = 0 \tag{13a}$$

$$\nabla_{\rho_3} E_3(\rho_3, \lambda_3; \rho_1, \frac{1}{2}\left(\rho_1(r - a(1,0,0)) + \rho_3(r + a(1,0,0))\right), \{\mathbf{R}_A\}) = 0 \tag{13b}$$

$$\lambda_1 = \lambda_3 \tag{13c}$$

$$\int_{D_1} \rho_1 dr + \int_{D_3} \rho_3 dr = \frac{2}{3} N_e \tag{13d}$$

which can be solved without referencing the second domain D_2. Note that no assumption is made about the charge neutrality in the domains; if an external nonsymmetric potential is present, the total charge will reflect the non-symmetry.

The condition in Eq.(13a) leads to the following integral equation, which must hold for any $\mathbf{r} \in D_1$:

$$\frac{5}{3} C_F \rho_1^{\frac{2}{3}}(\mathbf{r}) - \frac{4}{3} C_x \rho_1^{\frac{1}{3}}(\mathbf{r}) + \int_{D_1} \rho_1(\mathbf{r}') K_{11}(\mathbf{r}', \mathbf{r}) \mathrm{d}\mathbf{r}' + \int_{D_3} \rho_3(\mathbf{r}') K_{13}(\mathbf{r}', \mathbf{r}) \mathrm{d}\mathbf{r}' - \sum_{A=1}^{M} \frac{Z_A}{||\mathbf{r} - \mathbf{R}_A||} + \lambda_1 = 0 \tag{14a}$$

where the kernels K_{11} and K_{13} are defined as

$$K_{11} = \frac{1}{||\mathbf{r} - \mathbf{r}'||} + \frac{0.5}{||\mathbf{r} - (\mathbf{r}' + \mathbf{T})||} \qquad K_{13} = \frac{1}{||\mathbf{r} - \mathbf{r}'||} + \frac{0.5}{||\mathbf{r} - (\mathbf{r}' - \mathbf{T})||} \tag{14b}$$

where $\mathbf{T} = a(1,0,0)$. Similarly, writing the optimality condition of Eq.(13b) leads to the following integral equation, which must hold for any $\mathbf{r} \in D_3$:

$$\frac{5}{3} C_F \rho_3^{\frac{2}{3}}(\mathbf{r}) - \frac{4}{3} C_x \rho_3^{\frac{1}{3}}(\mathbf{r}) + \int_{D_1} \rho_1(\mathbf{r}') K_{31}(\mathbf{r}', \mathbf{r}) \mathrm{d}\mathbf{r}' + \int_{D_3} \rho_3(\mathbf{r}') K_{33}(\mathbf{r}', \mathbf{r}) \mathrm{d}\mathbf{r}' - \sum_{A=1}^{M} \frac{Z_A}{||\mathbf{r} - \mathbf{R}_A||} + \lambda_3 = 0 \tag{15a}$$

where the kernels K_{31} and K_{33} for this problem satisfy the condition

$$K_{31} = K_{11} \qquad K_{33} = K_{31} \tag{15b}$$

Equations 14a and 15a represent a set of nonlinear integral equations that are solved through standard techniques [2]. These equations were derived under the assumption that there is no deformation of the domains. However, similar equations can be derived from an interpolation approach on the underformed crystal, to which the problem on the deformed crystal is reduced by the composition $\rho \circ \Phi(\mathbf{r}^0, t)$, where $\Phi(\mathbf{r}^0, t)$ is the deformation mapping. In that case, Eq.(12) is replaced by

$$\rho_2(\mathbf{r}, t) = \rho_2(\Phi(\mathbf{r}^0, t)) \approx \frac{1}{2}\left(\rho_1(\Phi(\mathbf{r}^0 - \mathbf{T}, t)) + \rho_3(\Phi(\mathbf{r}^0 + \mathbf{T}, t))\right) \tag{16}$$

where the deformation Φ that depends on the position $\mathbf{r}^0$, of the point in the undeformed (material) frame, and time is as defined in section 1.1. The optimality condition $\nabla_{\rho_1} E_1 = 0$ leads to the following integral equation:

$$\frac{5}{3} C_F \rho_1^{\frac{2}{3}} - \frac{4}{3} C_x \rho_1^{\frac{1}{3}} + \int_{D_1} \frac{\rho_1(\mathbf{r}')}{||\mathbf{r} - \mathbf{r}'||} \mathrm{d}\mathbf{r}' + \int_{D_2} \frac{\rho_2(\mathbf{r}')}{||\mathbf{r} - \mathbf{r}'||} \mathrm{d}\mathbf{r}' + \int_{D_3} \frac{\rho_3(\mathbf{r}')}{||\mathbf{r} - \mathbf{r}'||} \mathrm{d}\mathbf{r}' - \sum_{A=1}^{M} \frac{Z_A}{||\mathbf{r} - \mathbf{r}'||} + \lambda_1 = 0 \tag{17}$$

A change of integration variable is performed to take the integration back to the undeformed domains:

$$\int_{D_1} \frac{\rho_1(\mathbf{r}')}{||\mathbf{r}-\mathbf{r}'||}\ \mathrm{d}\mathbf{r}' = \int_{D_1^0} \frac{\rho_1(\Phi(\mathbf{r}^{0\prime},t))}{||\Phi(\mathbf{r}^0,t)-\Phi(\mathbf{r}^{0\prime},t)||}\ |\mathbf{F}(\mathbf{r}^{0\prime},t)|\ \mathrm{d}\mathbf{r}^{0\prime} \tag{18a}$$

$$\int_{D_2} \frac{\rho_2(\mathbf{r}')}{||\mathbf{r}-\mathbf{r}'||}\ \mathrm{d}\mathbf{r}' = \int_{D_2^0} \frac{\rho_2(\Phi(\mathbf{r}^{0\prime},t))}{||\Phi(\mathbf{r}^0,t)-\Phi(\mathbf{r}^{0\prime},t)||}\ |\mathbf{F}(\mathbf{r}^{0\prime},t)|\ \mathrm{d}\mathbf{r}^{0\prime}$$

$$= \int_{D_2^0} \frac{0.5(\rho_1(\Phi(\mathbf{r}^{0\prime}-\mathbf{T},t))+\rho_3(\Phi(\mathbf{r}^{0\prime}+\mathbf{T},t)))}{||\Phi(\mathbf{r}^0,t)-\Phi(\mathbf{r}^{0\prime},t)||}\ |\mathbf{F}(\mathbf{r}^{0\prime},t)|\ \mathrm{d}\mathbf{r}^{0\prime} \tag{18b}$$

$$\int_{D_3} \frac{\rho_3(\mathbf{r}')}{||\mathbf{r}-\mathbf{r}'||}\ \mathrm{d}\mathbf{r}' = \int_{D_3^0} \frac{\rho_3(\Phi(\mathbf{r}^{0\prime},t))}{||\Phi(\mathbf{r}^0,t)-\Phi(\mathbf{r}^{0\prime},t)||}\ |\mathbf{F}(\mathbf{r}^{0\prime},t)|\ \mathrm{d}\mathbf{r}^{0\prime} \tag{18c}$$

Therefore, the optimality condition for any point $\mathbf{r}^0$ assumes the form of an integral equation:

$$\frac{5}{3}C_F\rho_1^{\frac{2}{3}}(\Phi(\mathbf{r}^0,t)) - \frac{4}{3}C_x\rho_1^{\frac{1}{3}}(\Phi(\mathbf{r}^0,t)) + \int_{D_1^0}\rho_1(\Phi(\mathbf{r}^{0\prime},t))K_{11}(\mathbf{r}^{0\prime},\mathbf{r}^0)\mathrm{d}\mathbf{r}^{0\prime} \tag{19a}$$

$$+\int_{D_3^0}\rho_3(\Phi(\mathbf{r}^{0\prime},t))K_{13}(\mathbf{r}^{0\prime},\mathbf{r}^0)\mathrm{d}\mathbf{r}^{0\prime} - \sum_{A=1}^{M}\frac{Z_A}{||\Phi(\mathbf{r}^0,t)-\Phi(\mathbf{R}_A^0,t)||} + \lambda_1 = 0$$

where the kernels K_{11} and K_{13} are defined as

$$K_{11}(\mathbf{r}^{0\prime},\mathbf{r}^0) = \frac{|\mathbf{F}(\mathbf{r}^{0\prime},t)|}{||\Phi(\mathbf{r}^0,t)-\Phi(\mathbf{r}^{0\prime},t)||} + \frac{0.5\ |\mathbf{F}(\mathbf{r}^{0\prime}+\mathbf{T},t)|}{||\Phi(\mathbf{r}^0,t)-\Phi(\mathbf{r}^{0\prime}+\mathbf{T},t)||} \tag{19b}$$

$$K_{13}(\mathbf{r}^{0\prime},\mathbf{r}^0) = \frac{|\mathbf{F}(\mathbf{r}^{0\prime},t)|}{||\Phi(\mathbf{r}^0,t)-\Phi(\mathbf{r}^{0\prime},t)||} + \frac{0.5\ |\mathbf{F}(\mathbf{r}^{0\prime}-\mathbf{T},t)|}{||\Phi(\mathbf{r}^0,t)-\Phi(\mathbf{r}^{0\prime}-\mathbf{T},t)||} \tag{19c}$$

$$\tag{19d}$$

Similarly, writing the optimality condition of Eq.(11) for domain D_3 leads to the following integral equation that must hold for any $\mathbf{r}^0$ in the undeformed domain D_3^0:

$$\frac{5}{3}C_F\rho_3^{\frac{2}{3}}(\Phi(\mathbf{r}^0,t)) - \frac{4}{3}C_x\rho_3^{\frac{1}{3}}(\Phi(\mathbf{r}^0,t)) + \int_{D_1^0}\rho_1(\Phi(\mathbf{r}^{0\prime},t))K_{31}(\mathbf{r}^{0\prime},\mathbf{r}^0)\mathrm{d}\mathbf{r}^{0\prime} \tag{20a}$$

$$+\int_{D_3^0}\rho_3(\Phi(\mathbf{r}^{0\prime},t))K_{33}(\mathbf{r}^{0\prime},\mathbf{r}^0)\mathrm{d}\mathbf{r}^{0\prime} - \sum_{A=1}^{M}\frac{Z_A}{||\Phi(\mathbf{r}^0,t)-\Phi(\mathbf{R}_A^0,t)||} + \lambda_3 = 0$$

where the kernels K_{31} and K_{33} satisfy

$$K_{31}(\mathbf{r}^{0\prime},\mathbf{r}^0) = K_{11}(\mathbf{r}^{0\prime},\mathbf{r}^0) \qquad K_{33}(\mathbf{r}^{0\prime},\mathbf{r}^0) = K_{31}(\mathbf{r}^{0\prime},\mathbf{r}^0) \tag{20b}$$

Note that Eqs.(19) and (20) are similar to Eqs.(14) and (15). The equations corresponding to the undeformed case are obtained by setting $|\mathbf{F}(\mathbf{r}^{0\prime},t)|=1$, and $\Phi(\mathbf{r}^0,t)=\mathbf{r}^0$ everywhere in $D_1^0\cup D_2^0\cup D_3^0$. These two conditions effectively indicate that none of these domains experiences any deformation.

In setting up and solving the above equations, an appropriate representation for $\Phi(\mathbf{r}^{0\prime},t)$ is necessary. In this work mesh-based representations are considered. This leads to the following representation:

$$\Phi(\mathbf{r}^{0\prime},t) = \sum_{A\in\mathcal{B}}\varphi(\mathbf{r}^{0\prime}|\mathbf{R}_A^0)\Phi(\mathbf{R}_A^0,t) \tag{21}$$

Thus, the deformation needs to be represented only at the points $\mathbf{R}_A^0,\ A\in\mathcal{B}$, and is then reconstructed by interpolation at the other points of the space, by using the shape functions $\varphi(\cdot,\cdot)$. The points $\mathbf{R}_A^0,\ A\in\mathcal{B}$ may or may not coincide with nuclear positions.

A difficulty with Eq.(19) is the fact that the equations are singular when $\mathbf{r}^0=\mathbf{R}_A^0$, $A=1,2,\ldots,M$, which raises the question whether the equations are well posed. Considering the procedure used to obtain these equations, one can only claim that they are valid everywhere except in small neighborhoods of the nuclear position; that is, not for $\mathbf{r^0}=\mathbf{R}_A^0$, $A=1,2,\ldots,M$. In addition, asymptotic examination (as $\mathbf{r^0}\to\mathbf{R}_A^0$, $A=1,2,\ldots,M$), of Eqs.(19) reveals that they can be asymptotically satisfied, provided that the leading term is

$$\rho\left(\Phi(\mathbf{r}^0,t)\right) \approx \left(\frac{3Z_A}{5C_F}\right)^{\frac{3}{2}}||\Phi(\mathbf{r}^0,t)-\Phi(\mathbf{R_A}^{0\prime})||^{-\frac{3}{2}} \tag{22a}$$

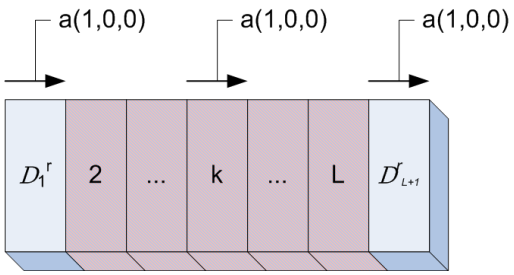

Figure 2: Electronic density reconstruction.

Since the above expression is integrable in three dimensions, it does not pose a problem for evaluating the total charge integral. In addition, this singularity is an artifact of the coordinate system used. Using spherical coordinates to represent the density around $\Phi(\mathbf{R}_A^{0\prime})$, the singularity is lifted by the determinant of the Jacobian of the coordinate transformation. With respect to those coordinates, the density satisfies

$$\rho\left(\Phi(\mathbf{r}^0,t)\right) \sim ||\Phi(\mathbf{r}^0,t) - \Phi(\mathbf{R_A}^{0\prime})||^{\frac{1}{2}} \tag{22b}$$

and the singularity is thus removed.

Nevertheless, this type of behavior is not easily captured on a computational mesh. A controlled approximation via smoothing of the potential will be introduced in section 2.3, and as a result the expression of the density will be numerically well behaved.

2.2 Analytic foundation of electronic density reconstruction

In this subsection, the process of electronic density reconstruction is referred to as fluctuation reconstruction, in reference to homogenization terminology [4]. The objective is to develop efficient tools that compute the solution to the electronic structure problem up to higher-order terms $\mathcal{O}\left(\mathbf{F}\right)^2 + \mathcal{O}\left(\nabla_0 \mathbf{F}\right)$. This is equivalent to carrying out the first step of the classical homogenization technique [4].

For simplicity, assume that two identical rectangular domains of linear size a are separated by a vector $La\,(1,0,0)$, where L is an integer. These *reference domains* $\mathcal{D}_1^r$ and $\mathcal{D}_{L+1}^r$, have electronic densities ρ_1 and ρ_{L+1}, respectively, that might have been computed by using an elaborate DFT method. The goal is to reconstruct the density in the domain between the two given rectangular domains (the shaded region in Fig.2). The notation convention $\mathbf{T}_k = k\mathbf{T}$ is used below.

The potential generated by the total charge in the system is

$$V(r) = \int \frac{\rho(r') + \rho_A(r')}{r - r'} dr'.$$

In our computations it is important to consider separately the potential that is generated by electronic density outside a given domain D, whose complement is $\bar{D}$, that is,

$$V^{ext}(r;D) = \int_{\bar{D}} \frac{\rho(r') + \rho_A(r')}{r - r'} dr' + \int_D \frac{\rho_A(r')}{r - r'} dr', \quad r \in D. \tag{23}$$

For solving the electronic problem, we may consider that the effect of the nuclei from the domain is also a part of an "external" potential, which explains the last term in the previous expression.

Clearly,

$$V(r) = V^{ext}(r;D)' + \int_D \frac{\rho(r')}{r - r'} dr'.$$

One consequence of the geometric assumption (see subsection 1.1) is that the external potential and the electronic density are nearly periodic, at least in the direction or in the region in which we do the reconstruction. For that assumption to be reasonable, one may imagine either that the domain depicted in Fig.2 is embedded in a crystal sufficiently large in the horizontal direction and periodic across, or that the end domains D_1^r and D_{L+1}^r are sufficiently far away from the boundary of the crystal. In addition, we assume that the "periodicity defect" is slowly varying in space on the scale of the domains.

This assumption is typical in homogenization theory, and in this context an observable $W(x)$ can be expressed as $W(x) = f(\frac{x}{b}, \frac{x}{a})$. Here $f(y,z)$ is a function that is periodic in z with a vector period $\hat{T} = O(1)$ and that is well behaved in y, that is, $\frac{\partial f}{\partial y} = O(1)$. An example of such function is $y\sin(z)$. Here a is the characteristic length scale of the fluctuations (the "microscale", or a measure of the domain D_1^r in our case, such as its diameter), whereas b is the "macroscale" length scale (in our case, the entire crystal or nanoparticle) and $a \ll b$.

As a result of our representation of $W(x)$, we have from the intermediate value theorem that, for any integer k, the following holds:

$$\left|W(x+k\widehat{T}a)-W(x)\right| = \left|f\left(\frac{x+k\widehat{T}a}{b},\frac{x+k\widehat{T}a}{a}\right)-f\left(\frac{x}{b},\frac{x}{a}\right)\right| = \left|f\left(\frac{x+k\widehat{T}a}{b},\frac{x}{a}\right)-f\left(\frac{x}{b},\frac{x}{a}\right)\right| = O\left(\frac{ka}{b}\right)$$

By a similar argument, the following also holds for nearly periodic $W(x)$.

$$\left(1-\tfrac{k-1}{L}\right)W(x)+\tfrac{k-1}{L}W\left(x+La\widehat{T}\right)-W\left(x+(k-1)a\widehat{T}\right)=O((L\tfrac{a}{b})^2),\quad k=1,2,\dots L+1$$

Therefore, the nearly periodic assumption for $V^{ext}(\mathbf{r};D)$ implies that the external potential has the following two properties

$$\begin{aligned}&\left|V^{ext}(\Phi\left(\mathbf{r}^0+\mathbf{T}_{k_1-1},t\right);D_{k_1})-V^{ext}\left(\Phi\left(\mathbf{r}^0+\mathbf{T}_{k_2-1},t\right);D_{k_2}\right)\right| \quad \leq \\ &O\left(\frac{(k_1-k_2)a}{b}\right)\leq O\left(\frac{La}{b}\right),\quad \forall \mathbf{r}^0\in D_1^r,\ 1\leq k_1<k_2<L+1,\end{aligned}$$

and

$$\begin{aligned}\left(1-\frac{k-1}{L}\right)V^{ext}(\Phi\left(\mathbf{r}^0,t\right);D_1) \quad &+ \quad \left(\frac{k-1}{L}\right)V^{ext}\left(\Phi\left(\mathbf{r}^0+\mathbf{T_L},t\right);D_{L+1}^r\right)\\ &- \quad V^{ext}\left(\Phi\left(\mathbf{r}^0+\mathbf{T}_{k-1},t\right);D_k\right)=O\left(\left(\frac{La}{b}\right)^2\right)k=1,2,\dots L+1,\ \mathbf{r}^0\in D_1^r\end{aligned}$$

In the following, we assess the error of reconstructing the electronic density in the domains D_k^r, $k=2,\dots,L$ by interpolation between its values in domains D_1^r and D_{L+1}^r. The reconstruction rule is the following:

$$\rho\left(\Phi\left(\mathbf{r}^0+\mathbf{T}_k\right),t\right)\approx\widehat{\rho}\left(\Phi\left(\mathbf{r}^0+\mathbf{T}_k,t\right)\right)=\left(1-\frac{k}{L}\right)\rho_1\left(\Phi\left(\mathbf{r}^0,t\right)\right)+\frac{k}{L}\rho_{L+1}\left(\Phi\left(\mathbf{r}^0+\mathbf{T}_L,t\right)\right),k=2,\dots L,\quad \mathbf{r}^0\in\mathcal{D}_1^r \tag{24}$$

where we have denoted

$$\rho_1\left(\Phi\left(\mathbf{r}^0,t\right)\right)=\rho\left(\Phi\left(\mathbf{r}^0,t\right)\right),\quad \rho_{L+1}\left(\Phi\left(\mathbf{r}^0+\mathbf{T}_L,t\right)\right)=\rho\left(\Phi\left(\mathbf{r}^0+\mathbf{T}_L,t\right)\right)\quad \mathbf{r}^0\in D_1^r$$

to emphasize the fact that the reconstructed density depends only on the density values.

Theorem 1 *Assume that the external potential is nearly periodic. Then the error in the optimality conditions of the electronic structure problem is*

$$O\left(\left(\frac{La}{b}\right)^2\right)+O\left(\rho_1\left(\Phi\left(\mathbf{r}^0,t\right)\right)-\rho_{L+1}\left(\Phi\left(\mathbf{r}^0+\mathbf{T}_L,t\right)\right)\right)^2$$

Proof
We now assume that the optimality conditions can be expressed as

$$\theta\left(\rho_k;V^{ext}(\Phi\left(\mathbf{r}^0+\mathbf{T_{k-1}},t\right);D_k);\mathbf{r}^0+\mathbf{T}_{k-1}\right)=0,\quad \mathbf{r}^0\in D_1^r,\ k=1,2,\dots,L+1,$$

where θ is an operator that is twice continuously differentiable in the range of approximation. For example, in the case of the Thomas-Fermi approach, Eq.(14) results in the following approach for θ.

$$\begin{aligned}\theta\left(\rho_k;V^{ext}\left(\Phi\left(\mathbf{r}^0+\mathbf{T}_{k-1},t\right);D_k\right);\mathbf{r}^0+\mathbf{T}_{k-1}\right)&=\frac{5}{3}C_F\rho_k^{\frac{2}{3}}\left(\Phi\left(\mathbf{r}^0+\mathbf{T}_{k-1},t\right)\right)-\frac{4}{3}C_x\rho_k^{\frac{1}{3}}\left(\Phi\left(\mathbf{r}^0+\mathbf{T}_{k-1},t\right)\right)\\ &+\int_{D_k}\frac{\rho_k(\Phi(\mathbf{r}^{0'},t))}{\Phi(\mathbf{r}^0+\mathbf{T}_{k-1},t)-\Phi\left(\mathbf{r}^{0'},t\right)}|\mathbf{F}(\mathbf{r}^{\mathbf{0}'},\mathbf{t})|\mathrm{d}\mathbf{r}^{0'}+V^{ext}\left(\Phi\left(\mathbf{r}^0+\mathbf{T}_{k-1},t\right);D_k^r\right)+\lambda=0\end{aligned}$$

where $\mathbf{r}^0\in D_1^r,\ k=1,2,\dots,L+1$. The second-order differentiability of θ holds as long as ρ is bounded from below.

In our approach, the reconstructed density depends only on the the values of the density in D_1^r and D_{L+1}^r, in which we assume that the optimality conditions are exactly satisfied, that is,

$$\theta\left(\rho_1;V^{ext}\left(\Phi\left(\mathbf{r}^0,t\right);D_1\right);\Phi\left(\mathbf{r}^0,t\right)\right)=0,\quad \theta\left(\rho_{L+1};V^{ext}\left(\Phi\left(\mathbf{r}^0+\mathbf{T}_L\right);D_{L+1}\right);\Phi\left(\mathbf{r}^0+\mathbf{T}_L\right)\right)=0,\quad \mathbf{r}^0\in D_1^r.$$

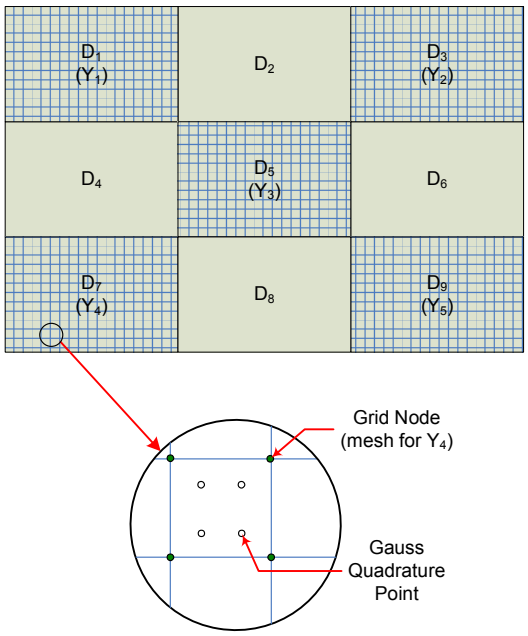

Figure 3: Nanostructure at end of *Preprocessing*.

Using analysis tools in interpolation theory, as well as the assumption that the external potential is nearly periodic, we obtain that

$$\theta\left(\widehat{\rho}\left(\Phi\left(\mathbf{r}^0+\mathbf{T}_k,t\right)\right),V^{ext}\left(\Phi\left(\mathbf{r}^0+\mathbf{T}_k,t\right);D_{k+1}\right),\left(\Phi\left(\mathbf{r}^0+\mathbf{T}_k,t\right)\right)\right)=$$
$$\theta\left(\left(1-\tfrac{k}{L}\right)\rho_1\left(\Phi\left(\mathbf{r}^0,t\right)\right)+\tfrac{k}{L}\rho_{L+1}\left(\Phi\left(\mathbf{r}^0+\mathbf{T}_L,t\right)\right),\left(1-\tfrac{k}{L}\right)V^{ext}\left(\Phi\left(\mathbf{r}^0\right);D_1^r\right)+\tfrac{k}{L}V^{ext}\left(\Phi\left(\mathbf{r}^0+\mathbf{T}_L,t\right);D_{L+1}^r\right)\right)+$$
$$O\left(\left(\tfrac{La}{b}\right)^2\right)=O\left(\left(\tfrac{La}{b}\right)^2\right)+O\left(\rho_1\left(\Phi\left(\mathbf{r}^0,t\right)\right)-\rho_{L+1}\left(\Phi\left(\mathbf{r}^0+\mathbf{T}_L,t\right)\right)^2\right),\quad \mathbf{r}^0\in D_1^r,\ k=1,2,\ldots,L-1,$$

which completes the proof.

The proposed interpolation-based approach has certain limitations and is not expected to always work well. In particular, the reconstructed density might display discontinuities at the interface between neighboring domains, which may be an issue with von Weizsacker-type kinetic energy corrections that are encountered in OF-DFT approaches [29]. However, for the purpose of generating just the field and computed the force on nuclei in the middle of the domain, the above approach is fairly accurate.

2.3 The strong form approach: the Thomas-Fermi example revisited

The strong form, or direct, approach refers to the case in which the electronic structure is computed, at least in some subdomains, by solving the system of integral equations that the first-order optimality condition leads to. In what follows this approach is exemplified for the Thomas-Fermi energy functional and applied to a domain $D=D_1\cup\ldots\cup D_u$ that contains the nanostructure. The optimality conditions of Eq.(11) are first formulated for a set of $p\leq u$ representative domains Y_1 through Y_p. In what follows, $Y=Y_1\cup\ldots\cup Y_p\subset D$; more precisely, there is an integer-to-integer mapping $\chi:\{1,\ldots,p\}\rightarrow\{1,\ldots,u\}$ such that $Y_j=D_{\chi(j)}$. The direct method computes the electronic density in Y and uses reconstruction by interpolation to recover ρ in $D-Y$. For instance, in Fig.1 there are three domains D_1, D_2, and D_3; $Y_1=D_1$, and $Y_2=D_3$. Likewise, in Fig.2 there are $L+1$ domains, but only two reconstruction domains: $Y_1=D_1$, and $Y_2=D_{L+1}$. Figure 3 also shows the partitioning of the domain D in which the electronic structure computation is carried out, as well as the reconstruction domains Y_1 through Y_5. The figure presents a two-dimensional case, but the discussion in this section covers both the two- and the three-dimensional case. By convention, in what follows Greek subscripts are used to index quantities associated with reconstruction domains.

At the core of the strong form approach stands the optimality condition for a generic domain $Y_\alpha\in Y$:

$$\frac{5}{3}C_F\rho_\alpha^{\frac{2}{3}}(\mathbf{r})-\frac{4}{3}C_x\rho_\alpha^{\frac{1}{3}}(\mathbf{r})+\sum_{i=1}^{u}\int_{D_i}\frac{\rho_i(\mathbf{r}')}{||\mathbf{r}-\mathbf{r}'||}\mathrm{d}\mathbf{r}'-\sum_{A=1}^{M}\frac{Z_A}{||\mathbf{r}-\mathbf{R}_A||}+\lambda=0 \tag{25}$$

The first step is to express the density ρ_i on domain D_i in terms of reference densities $\rho_\alpha \in Y_\alpha, \alpha \in \{1,\ldots,p\}$. A set of weights ϑ determined based on the type of interpolation considered (linear, quadratic, etc.) is used to this end:

$$\rho_i(\Phi(\mathbf{r}^{0\prime},t)) = \sum_{\alpha=1}^{p} \vartheta_\alpha(i)\rho_\alpha(\Phi(\mathbf{r}^{0\prime}+\mathbf{T}_{i\alpha},t)) \tag{26}$$

where the vector $\mathbf{T}_{i\alpha}$ is the translation vector that based on the periodicity assumption takes the point $\mathbf{r}^{0\prime}$ in domain D_i to its image in the domain Y_α.

Note that not all domains need to be included in the electronic density reconstruction. For example, if a domain has a defect, the electronic density is severly distorted away from near periodicity assumption, and should not be included in the reconstruction process in neibhboring domains. This can be formally accommodated by our approach by setting $v_\alpha(i) = \delta_{\alpha\chi(\alpha)}$, for such domains α where $\delta_{..}$ is the Kronecker symbol.

Taking into account the deformation of the structure,

$$\int_{D_i} \frac{\rho_i(\mathbf{r}')}{||\mathbf{r}-\mathbf{r}'||}\mathrm{d}\mathbf{r}' = \int_{D_i^0} \frac{\sum_{\alpha=1}^{p} \vartheta_\alpha(i)\rho_\alpha(\Phi(\mathbf{r}^{0\prime}+\mathbf{T}_{i\alpha},t))}{||\Phi(\mathbf{r}^0,t)-\Phi(\mathbf{r}^{0\prime},t)||} \ |\mathbf{F}(\mathbf{r}^{0\prime},t)| \ \mathrm{d}\mathbf{r}^{0\prime} = \sum_{\alpha=1}^{p} \int_{Y_\alpha^0} \rho_\alpha(\Phi(\mathbf{r}^{0\prime},t))\tilde{K}_{i\alpha}(\mathbf{r}^0,\mathbf{r}^{0\prime}) \ \mathrm{d}\mathbf{r}^{0\prime} \tag{27a}$$

$$\tilde{K}_{i\alpha}(\mathbf{r}^0,\mathbf{r}^{0\prime}) = \frac{\vartheta_\alpha(i) \ |\mathbf{F}(\mathbf{r}^{0\prime}-\mathbf{T}_{i\alpha},t)|}{||\Phi(\mathbf{r}^0,t)-\Phi(\mathbf{r}^{0\prime}-\mathbf{T}_{i\alpha},t)||} \tag{27b}$$

For any Y_α, Eq.(25) is reformulated as

$$\frac{5}{3}C_F\rho_\alpha^{\frac{2}{3}}(\Phi(\mathbf{r}^0,t))-\frac{4}{3}C_x\rho_\alpha^{\frac{1}{3}}(\Phi(\mathbf{r}^0,t))+\sum_{i=1}^{u}\left[\sum_{\gamma=1}^{p}\int_{Y_\gamma^0}\rho_\gamma(\Phi(\mathbf{r}^{0\prime},t)) \ \tilde{K}_{i\gamma}(\mathbf{r}^0,\mathbf{r}^{0\prime})\mathrm{d}\mathbf{r}^{0\prime}\right]-\sum_{A=1}^{M}\frac{Z_A}{||\Phi(\mathbf{r}^0,t)-\Phi(\mathbf{R}_A^0,t)||}+\lambda=0 \tag{28}$$

Defining for $\mathbf{r}^0 \in Y_\alpha^0$

$$K_{\alpha\gamma}(\mathbf{r}^0,\mathbf{r}^{0\prime}) = \sum_{i=1}^{u}\tilde{K}_{i\gamma}(\mathbf{r}^0,\mathbf{r}^{0\prime}) \tag{29a}$$

then Eq.(28) yields

$$\frac{5}{3}C_F\rho_\alpha^{\frac{2}{3}}(\Phi(\mathbf{r}^0,t)) - \frac{4}{3}C_x\rho_\alpha^{\frac{1}{3}}(\Phi(\mathbf{r}^0,t)) + \sum_{\gamma=1}^{p}\int_{Y_\gamma^0} K_{\alpha\gamma}(\mathbf{r}^0,\mathbf{r}^{0\prime})\rho_\gamma(\Phi(\mathbf{r}^{0\prime},t))\mathrm{d}\mathbf{r}^{0\prime} - \sum_{A=1}^{M}\frac{Z_A}{||\Phi(\mathbf{r}^0,t)-\Phi(\mathbf{R}_A^0,t)||}+\lambda=0 \tag{29b}$$

which should hold for any $\mathbf{r}^0 \in Y_\alpha$. Finally, since $\rho \geq 0$, a new function η is introduced such that

$$\rho(\Phi(\mathbf{r}^0,t)) = \eta^s(\mathbf{r}^0,t) \tag{30a}$$

where $s \geq 4$ is an even integer. This new function must then satisfy in the subdomain Y_α the following integral equations:

$$\frac{5}{3}C_F\eta_\alpha^{\frac{2s}{3}} - \frac{4}{3}C_x\eta_\alpha^{\frac{s}{3}} + \sum_{\gamma=1}^{p}\int_{Y_\gamma^0} K_{\alpha\gamma}(\mathbf{r}^0,\mathbf{r}^{0\prime})\eta_\gamma^s(\mathbf{r}^{0\prime},t)\mathrm{d}\mathbf{r}^{0\prime} - \sum_{A=1}^{M}\frac{Z_A}{||\Phi(\mathbf{r}^0,t)-\Phi(\mathbf{R}_A^0,t)||}+\lambda=0 \tag{30b}$$

The algorithm at this point calls for the solution of an nonlinear system of integral equations in ρ_α, $\alpha = 1,\ldots,p$. In order to solve this system, the reference domains Y_α are meshed by using hexahedrons. These meshes are denoted in what follows by $\mathcal{G}_1$ through $\mathcal{G}_p$, and they are associated with Y_1 through Y_p, respectively.

The direct numerical solution of the nonlinear system of integral equations becomes intractable in Cartesian coordinates because of the singularity when the grid points in a mesh $\mathcal{G}_\alpha$ approach a nuclei of location $\mathbf{R}_A$ (see Eq.(30b)). When approached in spherical coordinates in a three-dimensional representation this apparent singularity is in fact a nonissue (see the discussion related to Eq.(22)). Below, a potential-smoothing step is introduced to address the situation when $\mathbf{r}^0 \to \mathbf{R}_A^0$. Compared to the original term $||\Phi(\mathbf{r}^0,t)-\Phi(\mathbf{R}_A^0,t)||^{-1}$, the δ-smoothing function

$$\mathrm{S}_\delta(\mathbf{r}^0,\mathbf{R}_A^0,t) = \frac{1-e^{-\frac{||\Phi(\mathbf{r}^0,t)-\Phi(\mathbf{R}_A^0,t)||}{\delta}}}{||\Phi(\mathbf{r}^0,t)-\Phi(\mathbf{R}_A^0,t)||} \tag{31}$$

behaves similarly for large values of $||\Phi(\mathbf{r}^0,t)-\Phi(\mathbf{R}_A^0,t)||$ and δ small but positive, but it converges to $\frac{1}{\delta}$ rather than going to infinity when $\mathbf{r}^0 \to \mathbf{R}_A^0$. Thus, the smoothing process applied to Eq.(30b) leads to

$$\frac{5}{3}C_F\eta_\alpha^{\frac{2s}{3}} - \frac{4}{3}C_x\eta_\alpha^{\frac{s}{3}} + \sum_{\gamma=1}^{p}\int\limits_{Y_\gamma^0} K_{\alpha\gamma}(\mathbf{r}^0,\mathbf{r}^{0\prime})\eta_\gamma^s(\mathbf{r}^{0\prime},t)\mathrm{d}\mathbf{r}^{0\prime} - \sum_{A=1}^{M} Z_A\ \mathrm{S}_\delta(\mathbf{r}^0,\mathbf{R}_A^0,t) + \lambda = 0 \tag{32}$$

The following notation is used in what follows:

$\eta_{\beta j}$ – the value of η at the node j of grid $\mathcal{G}_\beta$

τ – a generic grid discretization cell of volume $||\tau||$

$\mathcal{V}(\tau)$ – the set of vertices associated with cell τ (four for a tetrahedron, eight for an hexahedron, etc.)

$|\mathcal{G}_\alpha|$ – the number of grid points in $\mathcal{G}_\alpha$

Y_γ^0 – undeformed reconstruction domain meshed with $\mathcal{G}_\gamma$; $Y_\gamma = \cup_{\tau\in\mathcal{G}_\gamma}\tau$

After discretization, the integral equation above yields at an arbitrary grid node $i \in \mathcal{G}_\alpha$ of location $\mathbf{r}_i^0 \in Y_\alpha$,

$$\frac{5}{3}C_F\eta_{\alpha i}^{\frac{2s}{3}} - \frac{4}{3}C_x\eta_{\alpha i}^{\frac{s}{3}} + \sum_{\gamma=1}^{p}\left[\sum_{\tau\in\mathcal{G}_\gamma}\int\limits_{\tau} K_{\alpha\gamma}(\mathbf{r}_i^0,\mathbf{r}^{0\prime})\ \eta_\gamma^s(\mathbf{r}^{0\prime},t)\mathrm{d}\mathbf{r}^{0\prime}\right] - \sum_{A=1}^{M} Z_A\ \mathrm{S}_\delta(\mathbf{r}_i^0,\mathbf{R}_A^0,t) + \lambda = 0 \tag{33}$$

The integral on τ is performed by q-point Gaussian numerical quadrature with weights w_l:

$$\int\limits_{\tau} K_{\alpha\gamma}(\mathbf{r}_i^0,\mathbf{r}^{0\prime})\ \eta_\gamma^s(\mathbf{r}^{0\prime},t)\mathrm{d}\mathbf{r}^{0\prime} \approx ||\tau||\ \sum_{l=1}^{q} w_l\ K_{\alpha\gamma}(\mathbf{r}_i^0,\mathbf{r}_l^{0\prime})\ \eta_\gamma^s(\mathbf{r}_l^{0\prime},t)$$

Figure 3 shows in the two-dimensional case a mesh cell and the quadrature points. As indicated in this figure, $\mathbf{r}_i^0$ describes the position of the grid nodes; the interior points (quadrature points) are located at $\mathbf{r}_l^{0\prime}$. The abscissas $\mathbf{r}_l^{0\prime}$ of the quadrature points are different from the mesh (grid) points, and the value of the unknown function η at these abscissas is obtained by interpolation. Interpolation at point $\mathbf{r}_l^{0\prime} \in \tau$, using a set of shape functions φ_d associated with the nodes $d \in \mathcal{V}(\tau)$, yields

$$\eta_\gamma^s(\mathbf{r}_l^{0\prime},t) \approx \sum_{d\in\mathcal{V}(\tau)} \eta_{\gamma d}^s\ \varphi_d(\mathbf{r}_l^{0\prime},t) = \sum_{d\in\mathcal{V}(\tau)} \eta_{\gamma d}^s\ \varphi_d^l$$

where φ_d^l are constants that can be precomputed. If one defines for $\mathbf{r}^0 \in Y_\alpha$ and $\mathbf{r}_l^{0\prime} \in Y_\gamma$

$$k_{\alpha\gamma d}(\mathbf{r}^0) = \sum_{l=1}^{q} w_l\ \varphi_d^l\ K_{\alpha\gamma}(\mathbf{r}^0,\mathbf{r}_l^{0\prime})\ , \tag{34a}$$

the discretized form of the integral equation expressed at grid node $i \in \mathcal{G}_\alpha$ of location $\mathbf{r}_i^0 \in Y_\alpha$ becomes

$$\frac{5}{3}C_F\eta_{\alpha i}^{\frac{2s}{3}} - \frac{4}{3}C_x\eta_{\alpha i}^{\frac{s}{3}} + \sum_{\gamma=1}^{p}\left[\sum_{\tau\in\mathcal{G}_\gamma} ||\tau|| \sum_{d\in\mathcal{V}} k_{\alpha\gamma d}(\mathbf{r}_i^0)\ \eta_{\gamma d}^s\right] - \sum_{A=1}^{M} Z_A\ \mathrm{S}_\delta(\mathbf{r}_i^0,\mathbf{R}_A^0,t) + \lambda = 0 \tag{34b}$$

Denoting the left side of Eq.(34b) by $\mathrm{P}_{\alpha i}(\eta)$, where $\eta = (\eta_{11},\eta_{12},\ldots,\eta_{p1},\eta_{p2},\ldots)^T$, the nonlinear system of equations that should be solved becomes

$$\mathrm{P}_{\alpha i}(\eta) = 0 \tag{35}$$

for $\alpha \in \{1,2,\ldots,p\},\ i = 1,\ldots,|\mathcal{G}_\alpha|$.

One additional equation is added to the set of $\sum_{\alpha=1}^{p}|\mathcal{G}_\alpha|$ equations above, and it follows from the charge constraint of Eq.(2b). The central idea is again to use the electronic density in the reference domains Y_α to express the electronic density in the whole domain D. Skipping the intermediary steps, this yields

$$\int\limits_{D} \rho(\mathbf{r})\mathrm{d}\mathbf{r} = \sum_{\alpha=1}^{p}\int\limits_{Y_\alpha^0} \eta_\alpha^s(\mathbf{r}^0,t)\hat{K}_\alpha(\mathbf{r}^0,t)\mathrm{d}\mathbf{r}^0 \tag{36a}$$

$$\hat{K}_\alpha(\mathbf{r}^0,t) = \sum_{i=1}^{u} \vartheta_\alpha(i)\ \ |\mathbf{F}(\mathbf{r}^0 - \mathbf{T}_{i\alpha},t)| \tag{36b}$$

Using for the evaluation of the integral on a cell of the undeformed grid Y_α^0 the same quadrature rule and interpolation method to evaluate the function at the quadrature points, the charge constraint equation eventually assumes the for

$$\sum_{\alpha=1}^{p}\left[\sum_{\tau\in Y_\alpha^0}\sum_{d\in\mathcal{V}(\tau)}\eta_{\alpha d}^{s}\hat{k}_{\alpha d}\right]-N_e=0 \tag{37a}$$

$$\hat{k}_{\alpha d}=\sum_{l=1}^{q}w_l\;\varphi_d^l\;\hat{K}_\alpha(\mathbf{r}_l^0,t) \tag{37b}$$

If a Newton-type method is considered for the solution of the nonlinear system of Eqs.(35) and (37a), the partials are computed as

$$\frac{\partial P_{\alpha i}}{\partial\eta_{\alpha i}}=\frac{10s}{9}C_F\eta_{\alpha i}^{\frac{2s-3}{3}}-\frac{4s}{9}C_x\eta_{\alpha i}^{\frac{s-3}{3}}+\sum_{\tau\in Y_\alpha^0}||\tau||\;\delta_{\tau i}^{\alpha}\;k_{\alpha\alpha i}(\mathbf{r}_i^0)\;\eta_{\alpha i}^{s-1} \tag{38a}$$

where $\delta_{\tau i}^{\alpha}=1$ if for $\tau\in\mathcal{G}_\alpha$, $i\in\mathcal{V}(\tau)$, and $\delta_{\tau i}^{\alpha}=0$ otherwise. When $i\neq j$ or $\alpha\neq\beta$,

$$\frac{\partial P_{\alpha i}}{\partial\eta_{\beta j}}=\sum_{\tau\in Y_\beta^0}||\tau||\;\delta_{\tau j}^{\beta}\;k_{\alpha\beta j}(\mathbf{r}_i^0)\;\eta_{\beta j}^{s-1} \tag{38b}$$

Likewise,

$$\frac{\partial P_{00}}{\partial\eta_{\beta j}}=\sum_{\alpha=1}^{p}\sum_{\tau\in Y_\alpha^0}s\;\eta_{\alpha d}^{s-1}\;\delta_{\tau d}^{\alpha}\;\hat{k}_{\alpha d} \tag{38c}$$

where, by convention, $P_{00}(\eta)$ is a notation for the left side of Eq.(37a).

3 DFT with density reconstruction

By reference to equation (29a), we define

$$\hat{K}_{\alpha\alpha}(\mathbf{r}^0,\mathbf{r}^{0\prime})=\sum_{i=1,\,i\neq\chi(\alpha)}^{u}\tilde{K}_{i\alpha}(\mathbf{r}^0,\mathbf{r}^{0\prime}),\;\mathbf{r}^0\in Y_\alpha^0. \tag{39}$$

It then follows that the external potential, as defined in (23), can be computed as

$$\begin{aligned}V^{ext}(r^0,\rho_1,\rho_2,\ldots,\rho_p,\alpha)\;&=\;\int_{Y_\alpha^0}\hat{K}_{\alpha\alpha}(\mathbf{r}^0,\mathbf{r}^{0\prime})\rho_\alpha(\Phi(\mathbf{r}^{0\prime},t))\mathrm{d}\mathbf{r}^{0\prime}+\sum_{\gamma=1,\gamma\neq\alpha}^{p}\int_{Y_\gamma^0}K_{\alpha\gamma}(\mathbf{r}^0,\mathbf{r}^{0\prime})\rho_\gamma(\Phi(\mathbf{r}^{0\prime},t))\mathrm{d}\mathbf{r}^{0\prime}\\&-\;\sum_{A=1}^{M}Z_A\;\mathrm{S}_\delta(\mathbf{r}^0,\mathbf{R}_A^0,t),\quad\alpha=1,2,\ldots,p,\;r^0\in Y_\alpha^0.\end{aligned} \tag{40}$$

Define now the following quantity

$$\mathcal{F}^{TF}(\rho_\alpha,\alpha)=\frac{5}{3}C_F\eta_\alpha^{\frac{2s}{3}}-\frac{4}{3}C_x\eta_\alpha^{\frac{s}{3}}+\int_{Y_\gamma^0}\tilde{K}_{\chi(\alpha)\alpha}(\mathbf{r}^0,\mathbf{r}^{0\prime})\rho_\gamma(\Phi(\mathbf{r}^{0\prime},t))\mathrm{d}\mathbf{r}^{0\prime}. \tag{41}$$

Then the optimality condition (29b) can be written as

$$\mathcal{F}^{TF}(\rho_\alpha,\alpha)+V^{ext}(r^0,\rho_1,\rho_2,\ldots,\rho_p,\alpha)+\lambda=0,\quad\alpha=1,2,\ldots,p,\;\mathbf{r}^0\in Y_\alpha^0.$$

The total charge density can also be computed based on (26)

$$\int\rho(r)dr=\sum_{i=1}^{u}\sum_{\alpha=1}^{p}\vartheta_\alpha(i)\int_{Y_\alpha^0}\rho_\alpha(\Phi(\mathbf{r}^{0\prime}+\mathbf{T}_{i\alpha},t))\left|F\left(\mathbf{r}^{0\prime}+\mathbf{T}_{i\alpha},t\right)\right|d\mathbf{r}^{0\prime}$$

With these notations, we note that our density reconstruction methodology applies irrespective of the particular DFT used. In that case, the only thing that changes is $\mathcal{F}^{KS}$. Therefore, the general electronic density problem with interpolation-based reconstruction becomes

$$\mathcal{F}(\rho_\alpha, \alpha) + V^{ext}(r^0, \rho_1, \rho_2, \ldots, \rho_p, \alpha) + \lambda = 0, \quad \alpha = 1, 2, \ldots, p, \ \mathbf{r}^0 \in Y^0_\alpha. \tag{42a}$$

$$\sum_{i=1}^{u} \sum_{\alpha=1}^{p} \vartheta_\alpha(i) \int_{Y^0_\alpha} \rho_\alpha(\Phi(\mathbf{r}^{0\prime} + \mathbf{T}_{i\alpha}, t)) \left| F\left(\mathbf{r}^{0\prime} + \mathbf{T}_{i\alpha}, t\right) \right| d\mathbf{r}^{0\prime} = N. \tag{42b}$$

An useful fact is that $\mathcal{F}(\rho_\alpha, \alpha)$ is the gradient of the objective function of the electronic structure problem on domain D_α, $\alpha = 1, 2, \ldots, p$. We can therefore use, for a given DFT approach, any software that returns the gradient with respect to ρ of the energy functional on domain D_α, coupled with a quasi-Newton approach to solve (42).

3.1 Nonlinear equations vs. optimization approaches

The above problem is a nonlinear equation, that originates in an optimization problem. It can be immediately proven that, in aggregate, it does not represent the first-order conditions of an optimization problem. That issue is a bit unsettling, since solving optimization problems is typically a more robust process than solving equivalent nonlinear equations, because any local minimum of the optimization problem satisfies the nonlinear equation of its optimality conditions. When only a nonlinear system is available, a local minimum of the residual is not necessarily a solution of the nonlinear system.

It is therefore important to assess whether there exists an optimization problem that is equivalent, at least up to leading order of the homogenization error (La/b) with the nonlinear system.

In an abstract formulation, we have the following problem.

$$\min_{x_1, x_2} \ f(x_1, x_2)$$

Here we assume that the variables x_1 correspond to the representative degrees of freedom whereas x_2 correspond to the rest of the degrees of freedom. In the electronic problem with density reconstruction, the representative degrees of freedom are the ones used to parametrize the electronic density in the representative domains D_α, $\alpha = 1, 2, \ldots, p$. In the quasi continuum method , the representative degrees of freedom are the positions of the repatoms [26]. The latter method is based on the observation that one expects at the solution to have $x_2 = T(x_1)$ where $T(x_1)$ is the piecewise linear interpolation mapping with nodes at the repatoms. In the electronic density problem, the mapping $T(\cdot)$ is the interpolation-based operator from (26).

Based on this observation, one can formulate the nonlinear equation

$$\nabla_{x_1} \ f(x_1, x_2), \ x_2 = T(x_1)$$

which will provide the same solution as the original problem. However, the problem is an equilibrium problem with equilibrium constraints rather than a minimization problem.

However, it immediately results using the chain rule that the optimization problem

$$\min_{x_1} f(x_1, T(x_1)),$$

has the same solution as the previous two, provided that the reduced Hessian is positive definite, which should be true if the original Hessian was positive definite, and the interpolation mapping is full rank. This observation presents the advantage that one solves an optimization problem as opposed to a system of nonlinear equations, and one has a better global convergence safeguards for the situation, which should help for the case when there are many local minima to avoid the points that do not have the correct inertia of the Hessian.

In our case the first approach is the "optimize-and-interpolate" approach that we described in Section (2), whereas the second approach is the "interpolate-and-optimize" approach that we describe in the Subsection 3.2 bellow . The following result settles in the positive the question of whether the two approaches are equivalent in the limit of the ansatz $x_2 = T(x_1)$. The proof technique is similar to the one we used for proving the approximation order of the interpolation approach, and is ommited.

Theorem 2 *Assume that the solution $x^* = (x_1^*, x_2^*)$ of the original optimization problem satisfies $\|x_2^* - T(x_1^*)\| \ll 1$, therefore the multiscale ansatz is not perfect, it is merely very good. Then the solution $\tilde{x}_1$ of the nonlinear equation and $\hat{x}_1$ of the reduced optimization problem satisfy*

$$\|x_1^* - \tilde{x}_1\| = O(\|x_2^* - T(x_1^*)\|^2) \quad \|x_1^* - \hat{x}_1\| = O(\|x_2^* - T(x_1^*)\|^2)$$

3.2 An optimization approach for the electronic structure problem

In this section we discuss the approach in which we use the interpolation ansatz (26) to create a reduced energy functional, that depends only on the densities in the representative domains, which we then minimize.

The key terms are the ones that emerge from the electrostatic potential. We present a succint derivation of the respective equations.

Define

$$\begin{aligned}
\tilde{K}_{\alpha\gamma}(\mathbf{r}^0,\mathbf{r}^{0'}) &= \sum_{i=1}^{u}\sum_{j=1}^{u} v_\alpha(i)v_\gamma(j)\frac{\left|F(\mathbf{r}^0+\mathbf{T}_{\chi(\alpha),i},t)\right|\left|F(\mathbf{r}^{0'}+\mathbf{T}_{\chi(\gamma),j},t)\right|}{||\Phi(\mathbf{r}^0+\mathbf{T}_{\chi(\alpha),i},t)-\Phi(\mathbf{r}^{0'}+\mathbf{T}_{\chi(\gamma),j},t)||}, \quad \alpha,\gamma=1,2,\ldots,p,\ \mathbf{r}^0\in Y_\alpha^0\,\mathbf{r}^{0'}\in Y_\gamma^0,\\
\tilde{L}_\alpha(\mathbf{r}^0) &= \sum_{A=1}^{M}\sum_{i=1}^{u} v_\alpha(i)\frac{\left|F(\mathbf{r}^0+\mathbf{T}_{\chi(\alpha),i},t)\right|}{||\Phi(\mathbf{r}^0+\mathbf{T}_{\chi(\alpha),i},t)-\Phi(\mathbf{R}_A,t)||}, \quad \alpha=1,2,\ldots,p,\mathbf{r}^0\in Y_\alpha^0,\\
\tilde{M}_\alpha(\mathbf{r}^0) &= \sum_{i=1}^{u} v_\alpha(i)\left|F(\mathbf{r}^0+\mathbf{T}_{\chi(\alpha),i},t)\right| \quad \alpha=1,2,\ldots,p\ \mathbf{r}^0\in Y_\alpha^0.
\end{aligned}$$

Using the interpolation ansatz, we can express several of the terms in (7) as a function of the densities in the representative domains.

$$\begin{aligned}
J(\rho) &= \frac{1}{2}\sum_{\alpha=1}^{p}\sum_{\gamma=1}^{p}\int_{Y_\alpha^0}\int_{Y_\gamma^0}\tilde{K}_{\alpha\gamma}(\mathbf{r}^0,\mathbf{r}^{0'})\rho_\alpha(\Phi(\mathbf{r}^0,t))\rho_\gamma(\Phi(\mathbf{r}^{0'},t))d\mathbf{r}^0 d\mathbf{r}^{0'}\\
E_{ne}(\rho) &= -\sum_{\alpha=1}^{p}\int_{Y_\alpha^0}\tilde{L}_\alpha(\mathbf{r}^0)\rho_\alpha(\Phi(\mathbf{r}^0,t))d\mathbf{r}^0,\\
\int\rho d\mathbf{r} &= \sum_{\alpha=1}^{p}\int_{Y_\alpha^0}\tilde{M}_\alpha(\mathbf{r}^0)\rho_\alpha(\Phi(\mathbf{r}^0,t))d\mathbf{r}^0.
\end{aligned}$$

The difficult part has to do with the kinetic energy and exchange terms $T[\rho]$, $K[\rho]$ whose dependence on the density is not linear and, outside the Thomas-Fermi theory, not even simple to state. Assume that the latter terms are described by a univariate density $\theta^1(\rho,r)$, as described in the first term of (1), and as is indeed the case for the Thomas-Fermi representation, with rhe rule

$$\theta^1(\rho,r)=C_F\rho^{\frac{5}{3}}-C_x\rho^{\frac{4}{3}}.$$

Then, by an argument similar to the one in Theorem 1, we obtain that the following approximation is accurate, up to terms $O((\frac{La}{b})^2)$.

$$T[\rho]+K[\rho]\approx\sum_{\alpha=1}^{p}\int_{Y_\alpha^0}\tilde{M}_\alpha(\mathbf{r}^0)\theta^1(\rho_\alpha,\Phi(\mathbf{r}^0,t))d\mathbf{r}^0.$$

With these approximations and definitions and referring back to (7) we can then define the following electronic structure computation problem

$$\min E^{IO}(\rho),\quad \text{subject to}\ \int\rho=N, \tag{43}$$

where we use the superscript "IO" to denote the "interpolate-and-optimize" approach.

The following are the optimality conditions of the optimality conditions.

$$\begin{aligned}
0 &= \tilde{M}_\alpha(\mathbf{r}^0)\nabla_\rho\theta^1(\rho_\alpha,\Phi(\mathbf{r}^0,t))-\tilde{L}_\alpha(\mathbf{r}^0)+\sum_{\gamma=1}^{p}\int_{Y_\gamma^0}\tilde{K}_{\alpha\gamma}(\mathbf{r}^0,\mathbf{r}^{0'})\rho_\gamma(\Phi(\mathbf{r}^{0'},t))d\mathbf{r}^{0'}+\lambda\tilde{M}_\alpha(\mathbf{r}^0)\\
N &= \sum_{\gamma=1}^{p}\int_{Y_\gamma^0}\tilde{M}_\alpha(\mathbf{r}^0).
\end{aligned}$$

It is clear that the optimality conditions of the "interpolate-and-optimize" approach are more computationally intensive to set up. Nonetheless, they open the avenue for using special techniques (such as projected gradient) that are available and stable only for optimization formulation. We plan to compare the relative benefits of the "interpolate-and-optimize" approach versus the "optimize-and-interpolate approach" in the near future.

4 Nanostructure Shape Investigation

The optimization of the geometry of a nanostructure, to find the most stable shape, reduces to solving an optimization problem (called hereafter the *Ionic Problem*) that minimizes the total energy given an electronic ground state configuration of energy E_e as a function of the position of the nuclei. More precisely, the equilibrium configuration of a nanostructure is provided by that distribution of the nuclei that minimizes the energy

$$E_{tot} = E_e + E_{nn} \ , \tag{44}$$

where E_{nn} is the nucleus-nucleus interaction energy.

The assumption is that the kinetic energy of the nuclei is zero and, central to this development, that E_e is the electronic ground-state energy for the considered nuclear distribution. Following the Born-Oppenheimer assumption, the electronic energy depends parametrically on the positions of the nuclei, through the dependence of the electronic density on the nuclei positions. Thus, in a general from (that has the Thomas-Fermi of Eq.(7) as a subcase):

$$E_e = T[\rho(\mathbf{r})] + E^{Har}[\rho(\mathbf{r})] + E^{xc}[\rho(\mathbf{r})] + \int \rho(\mathbf{r})\, V_{ext}(\mathbf{r}; \{\mathbf{R}_A\})\, \mathrm{d}\mathbf{r} \ , \tag{45}$$

where $T[\rho(\mathbf{r})]$ is the kinetic energy functional, $E^{Har}[\rho(\mathbf{r})]$ is the electron-electron Coulomb repulsion energy, $E^{xc}[\rho(\mathbf{r})]$ is the exchange and correlation energy, and $V_{ext}(\mathbf{r}; \{\mathbf{R}_A\})$ is the ionic potential, which parametrically depends on the distribution of the nuclei $\{\mathbf{R}_A\}$. The explicit dependence of $T[\rho(\mathbf{r})]$ and $E^{xc}[\rho(\mathbf{r})]$ on the density $\rho(\mathbf{r})$ is typically not available, and consequently it is approximated in some fashion [22, 29, 23, 13], an issue beyond the scope of this document. According to the Hohenberg-Kohn theorem [14], the electronic density is such that it minimizes E_e subject to the charge conservation constraint of Eq.(2b).

Theorem 3 *Consider the optimization problem*

$$\min_{\{\mathbf{R}_A\}} E_{tot} = E_e + E_{nn} \tag{46a}$$

subject to the constraint that for a nuclear configuration $\{\mathbf{R}_A\}$ the energy E_e is the electronic ground-state energy, and the electronic density $\hat{\rho}$ that realizes this electronic ground energy additionally satisfies the charge constraint equation of Eq.(2b). Under these assumptions, the first order optimality conditions for the optimization problem of Eq.(46a) lead to

$$\mathbf{F}_K = \frac{\partial E_{ext}}{\partial \mathbf{R}_K} + \frac{\partial E_{nn}}{\partial \mathbf{R}_K} = \mathbf{0} \ , \tag{46b}$$

where $\mathbf{F}_K$ is interpreted as the force acting on nucleus K, and by definition

$$E_{ext}(\mathbf{r}; \{\mathbf{R}_A\}) = -\sum_{A=1}^{M} \int \hat{\rho}(\mathbf{r})\, V_{ext}\left(\mathbf{r}; \{\mathbf{R}_A\}\right) d\mathbf{r} = -\sum_{A=1}^{M} \int \frac{Z_A \hat{\rho}(\mathbf{r})}{|\mathbf{r} - \mathbf{R}_A|}\, d\mathbf{r} \tag{46c}$$

$$E_{nn} = \frac{1}{2} \sum_{A=1}^{M} \sum_{B=A+1}^{M} \frac{Z_A Z_B}{\mathbf{R}_{AB}} \ . \tag{46d}$$

Proof

The proof relies on the calculus of variations. Since $\hat{\rho}(\mathbf{r})$ is determined to minimize the electronic energy, there is a parametric dependency of this value on the ionic position: $\hat{\rho}(\mathbf{r}) = \rho(\mathbf{r}; \{\mathbf{R}_A\})$. After application of the chain rule, the optimality conditions for E_{tot} will read

$$\frac{\delta E_e}{\delta \rho} \frac{\partial \rho}{\partial \mathbf{R}_K} + \frac{\partial E_e}{\partial \mathbf{R}_K} + \frac{\partial E_{nn}}{\partial \mathbf{R}_K} = 0 \tag{47}$$

where $\mathbf{R}_K$ is the position of an arbitrary nucleus K.

The optimality conditions for minimizing the electronic energy as a functional of the electronic density lead to

$$\frac{\delta E_e}{\delta \rho} + \lambda \frac{\delta g}{\delta \rho} = 0 \ , \tag{48}$$

where λ is the Lagrange multiplier associated with the constraint

$$g[\rho] = 0 \tag{49}$$

that the electronic density must satisfy. For the problem at hand the charge conservation equation results in $g[\rho] = \int \rho(\mathbf{r})\, \mathrm{d}\mathbf{r} - N_e$. Based on Eq.(49), the variation of $\rho(\mathbf{r})$ with respect to $\mathbf{R}_k$ must satisfy

$$\frac{\delta g}{\delta \rho} \frac{\partial \rho}{\partial \mathbf{R}_K} = 0 \ .$$

Multiplying Eq.(48) from the right by $\frac{\partial \rho}{\partial \mathbf{R}_K}$ leads to $\frac{\delta E_e}{\delta \rho} \frac{\partial \rho}{\partial \mathbf{R}_K} = 0$, which, substituted back into (47) yields the optimality condition stated in Eq.(46b) and thus completes the proof.

Therefore, for each nucleus K in the system, Eq.(46b) leads to the condition

$$\int \hat{\rho}(\mathbf{r}) \frac{\mathbf{r} - \mathbf{R}_K}{||\mathbf{r} - \mathbf{R}_K||^{\frac{3}{2}}} \, \mathrm{d}\mathbf{r} + \sum_{A=1, A \neq K}^{M} Z_A \frac{\mathbf{R}_A - \mathbf{R}_K}{||\mathbf{R}_A - \mathbf{R}_K||^{\frac{3}{2}}} = \mathbf{0} \, . \tag{50}$$

Remarks:

1. The value of the above theorem is that it allows us to solve the nuclear equilibrium problem by using only the solution of the electronic density problem, and not the values and the derivatives of the kinetic and exchange energy functionals. Therefore, we can use even an entirely nontransparent encapsulation of the electronic structure problem which allows our approach to work well with legacy codes that do not provide all the needed derivatives.
2. The key observation is that once the electronic density is available, the equilibrium conditions of Eq.(50) can be imposed right away. Wether the electronic structure computation is done with KS-DFT or OF-DFT is irrelevant; moreover, there is no need to know the explicit dependence of the energy E_e on the electronic density $\rho(\mathbf{r})$.
3. As suggested in [19], the one-atom conditions of Eq.(46b) can be replaced by cluster conditions, an alternative that will be explored in the future.
4. Because of the presence of the electronic density $\rho(\mathbf{r})$ that displays pronounced cusps in the vicinity of nuclei, the integral in Eq.(50) must be evaluated by using special techniques [3, 28]. This computational aspect is central to the overall algorithm and will be detailed in a separate document.

When a local quasicontinuum approach is used, the condition of Eq.(50) is imposed only for *repnuclei*; that is, only for $K \in \mathcal{B}$ (see Eq.(21)). The position of the rest of the atoms in the system is then expressed in terms of the position of the *repnuclei*. The *repnuclei* become the nodes of an atomic mesh, and interpolation is used to recover the position of the remaining nuclei. For instance, if the atomic mesh is denoted by $\mathcal{M}$, τ is an arbitrary cell in this mesh, $\mathcal{V}(\tau)$ represents the set of the nodes associated with cell τ, and φ_L is the shape function associated with node L, then the condition of Eq.(50) is approximated as

$$\int \hat{\rho}(\mathbf{r}) \frac{\mathbf{r} - \mathbf{R}_K}{||\mathbf{r} - \mathbf{R}_K||^{\frac{3}{2}}} \, \mathrm{d}\mathbf{r} + \sum_{\tau \in \mathcal{M}} \sum_{A \in \tau} Z_A \frac{\sum\limits_{L \in \mathcal{V}(\tau)} \mathbf{R}_L \varphi_L(\mathbf{R}_A) - \mathbf{R}_K}{|| \sum\limits_{L \in \mathcal{V}(\tau)} \mathbf{R}_L \varphi_L(\mathbf{R}_A) - \mathbf{R}_K||^{\frac{3}{2}}} = \mathbf{0} \, . \tag{51}$$

This effectively reduces the dimension of the problem from $3\,M$ (the (x, y, z) coordinates of the nuclei), to $3\,M_{rep}$, where M_{rep} is the number of nodes in the atomic mesh (the number of *repnuclei*). The sum in Eq.(51) is most likely not going to be the simulation bottleneck (solving the electronic problem for $\hat{\rho}$ is significantly more demanding), but fast-multipole methods [1, 11, 24] can be considered to speed the summation.

Denoting by $\mathbf{P}_i$, $i = 1, \ldots, M_{rep}$, the position of the representative nucleus n_i, the set of nonlinear equations of Eq.(51) can be grouped into a nonlinear system that is solved for the relaxed configuration of the structure.

$$\begin{aligned} &\mathbf{f}_1(\mathbf{P}_1, \mathbf{P}_2, \ldots \mathbf{P}_{M_{rep}}) = \mathbf{0} \\ &\mathbf{f}_2(\mathbf{P}_1, \mathbf{P}_2, \ldots \mathbf{P}_{M_{rep}}) = \mathbf{0} \\ &\ldots \\ &\mathbf{f}_{M_{rep}}(\mathbf{P}_1, \mathbf{P}_2, \ldots \mathbf{P}_{M_{rep}}) = \mathbf{0} \end{aligned} \tag{52}$$

Finding the solution of this system is done by a Newton-like method. Evaluating the Jacobian information is straightforward but not detailed here.

Finally, note that within Eq.(51) a connection is made back to Eq.(21); the position of an arbitrary nucleus A in cell τ is computed based on interpolation using the nodes $\mathcal{V}(\tau)$, one of many alternatives available (one could consider *repnuclei* from neighboring cells for instance). Effectively, this provides in Eq.(21) an expression for $\Phi(\cdot, t)$ that only depends on $A \in \mathcal{V}(\tau)$ rather than $A \in \mathcal{B}$.

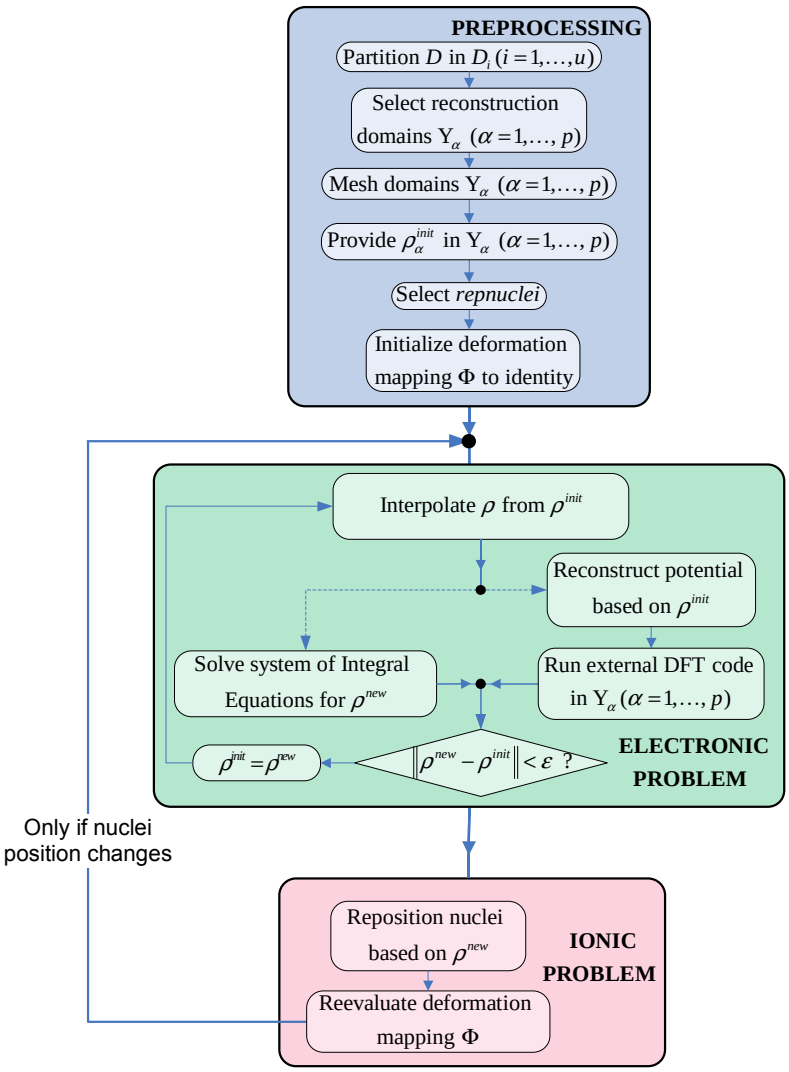

Figure 4: Computational flow.

5 Proposed Computational Setup

Given a nanostructure of known atomic composition (not necessarily mono-atomic or single-crystal), the goal is to determine the electron density distribution as well as its final configuration; that is, the mapping Φ. Because of the assumption that the kinetic energy of the nuclei is zero, the problem corresponds to a zero Kelvin temperature scenario. A methodology that handles the non-zero temperature case is not addressed here; most likely, it would follow an approach similar to that of Car-Parrinello [5], or Payne et al. [21].

As indicated in Fig.4, the proposed solution has three principal modules: the *Preprocessing* stage, the *Electronic Problem*, and the *Ionic Problem*. *Preprocessing* is carried out once at the beginning of the simulation. A suitable chosen domain D is selected to include the nanostructure investigated. The partitioning of D into u subdomains $D_i, i = 1, \ldots, u$, is done to mirror the underlying periodicity of the structure. A set of subdomains $D_{\chi(1)}$ through $D_{\chi(p)}$ is determined to constitute the reconstruction domains, and as in section 2.3 they are denoted by Y_1 through Y_p. In these p subdomains explicit electronic structure computation will be carried out accurately. A set of values of the electronic density is required at the nodes of the discretization mesh; the initial guess for the electronic density could be a uniform distribution throughout the nanostructure or, when practical, could be obtained based on a periodic boundary conditions assumption by computing it in a domain D_j and then cloning for the remaining domains D_k. *Preprocessing* concludes with the initialization of the deformation map Φ to zero.

The *Electronic Problem* can be solved externally or internally. When it is solved externally, a specialized code such as NWChem [12] or Gaussian03 [9] is employed to compute the electronic density in the reconstruction subdomains $Y_\alpha, \alpha \in \{1, \ldots, p\}$. When the electronic problem is solved internally (only for qualitative studies,

using for instance the Thomas-Fermi DFT; see section 2.3), the electronic structure computation requires a mesh grid on which the integrals associated with the formulation are discretized. The algorithm uses three-dimensional interpolation to provide for the density in D_j, where $j \in \{1, \ldots, u\} - \{\chi(1), \ldots, \chi(p)\}$ (the analytical basis of this process is detailed in section 2).

Independent of the type of solver invoked (external or internal), with a suitable norm the new electronic density ρ^{new} is compared to ρ^{init}, and the computation restarts the *Electronic Problem* after setting $\rho^{init} = \rho^{new}$, unless the corrected and initial values of the electronic density are close. This iterative process constitutes the first inner loop of the algorithm. Its analytical foundation is discussed in sections 2 and 3.

The *Ionic Problem* uses the newly computed electronic density to reposition the nuclei and thus alter the shape of the structure. The nonlinear system of Eq.(52) provides the position of the *repnuclei*, the other nuclei being positioned based on the quasi-continuum paradigm discussed in section 4. The nonlinear system in Eq.(52) is used by an iterative method, which leads to the second computation inner loop. This second inner loop has four steps:

1. Evaluate the integral of Eq.(51); when necessary, evaluate its partial with respect to $\mathbf{P}_i$
2. Evaluate the double sum of Eq.(51), which is based on a partitioning of the structure; when necessary, evaluate its partial with respect to the position of the representative atoms
3. Carry out a quasi-Newton step to update the positions $\mathbf{P}_i$ of the M_{rep} representative nuclei.
4. Go back to 1 if not converged

The precision in determining the position of the nuclei is directly influenced by the accuracy of the electronic density $\rho(\mathbf{r})$. Accurately solving the *Electronic Problem* is computationally intensive, and thus an important issue not addressed by this work is the sensitivity of the solution of the non-linear system of Eq.(52) with respect to $\rho(\mathbf{r})$. It remains to be determined weather a crude approximation of the electronic density suffices for solving the *Ionic Problem* at a satisfactory level of accuracy.

After determining the position of the nuclei, the algorithm computes the new deformation mapping Φ according to Eq.(21). If the overall change in the position of *repnuclei* at the end of the *Ionic Problem* is smaller than a threshold value, the computation stops; otherwise the new distribution of the nuclei is the input to a new *Electronic Problem* (second stage of the algorithm).

In summary, the algorithm passes through the *Preprocessing* stage once. It then solves the *Electronic Problem* (the first inner loop) and proceeds to the *Ionic Problem* (the second inner loop). The outer loop (*Electronic Problem*, followed by *Ionic Problem*) stops when there is no significant change in the position of the *repnuclei*.

6 Conclusions

This paper proposes a theoretical framework for nanostructure optimization. The *geometric* (space periodicity), and the *electronic* (energy functional form) assumptions introduced in section 1.1 are at the center of a methodology that uses interpolation and coupled cross-domain optimization techniques in an effort to increase the size of the problems that rely on a DFT-based solution component. For the electron density computation (the *Electronic Problem*) formal error bounds are provided for the interpolation and cross-domain reconstruction techniques used. The electronic density reconstruction process can be done internally following an approach similar to the one introduced in section 2.3 for the Thomas-Fermi DFT; alternatively, it can be carried out using dedicated third party software such as NWChem or Gaussian03. In either case, the density is reconstructed by solving a cross-domain coupled nonlinear problem formulated in section 3 as an optimization problem. The last step of the proposed methodology calls for solving the *Ionic Problem*; that is, repositioning the nuclei of the structure given the electronic density in the domain. It was shown in section 4 that the new ionic configuration is the solution of a non-linear system obtained based on a first order optimality condition. The Jacobian information for this system is readily available, and its solution does not require the explicit dependency of the kinetic and exchange-correlation energies on the electronic density.

Based on the proposed methodology, a set of simple test cases are currently under investigation: (a) the test case presented in Fig.1 for a mono-atomic Al structure bounded by a surface; (b) the electronic structure study of an inner defect in a silicon crystal.

7 Acknowledgement

This work was supported in part by the Mathematical, Information, and Computational Sciences Division subprogram of the Office of Advanced Scientific Computing Research, Office of Science, U.S. Department of Energy, under Contract W-31-109-ENG-38.

This work was supported in part by the U.S. Department of Energy, Office of Basic Energy Sciences-Materials Sciences, under Contract No. W-31-109-ENG-38.

References

[1] A. W. Appel, *An efficient program for many-body simulation*, J. Sci. Stat. Comput., 6 (1985), pp. 85–103.

[2] C. T. H. Baker, *The numerical treatment of integral equations*, Clarendon Press, Oxford, 1977.

[3] A. D. Becke, *A multicenter numerical integration scheme for polyatomic molecules*, The Journal of Chemical Physics, 88 (1988), pp. 2547–2553.

[4] A. Bensoussan, J.-L. Lions, and G. Papanicolaou, *Asymptotic analysis for periodic structures*, vol. 5 of Studies in Mathematics and its Applications, North-Holland Publishing Co., Amsterdam-New York, 1978.

[5] R. Car and M. Parrinello, *Unified approach for molecular dynamics and density-functional theory*, Phys. Rev. Lett., 55 (1985), p. 2471.

[6] A. Conn, N. Gould, and P. Toint, *LANCELOT: A Fortran package for large-scale nonlinear optimization*, Springer-Verlag, New York, 1992.

[7] M. Fago, R. L. Hayes, E. A. Carter, and M. Ortiz, *Density-functional-based local quasicontinuum method: prediction of dislocation nucleation*, Phys. Rev., **B70** (2004), pp. 100102:1–4.

[8] E. Fermi, *Un metodo statistice per la determinazione di alcune proprieta dell'atomo*, Rend. Accad. Lincei, **6** (1927), pp. 602–607.

[9] M. J. Frisch, G. W. Trucks, H. B. Schlegel, G. E. Scuseria, M. A. Robb, J. R. Cheeseman, J. A. Montgomery, Jr., T. Vreven, K. N. Kudin, J. C. Burant, J. M. Millam, S. S. Iyengar, J. Tomasi, V. Barone, B. Mennucci, M. Cossi, G. Scalmani, N. Rega, G. A. Petersson, H. Nakatsuji, M. Hada, M. Ehara, K. Toyota, R. Fukuda, J. Hasegawa, M. Ishida, T. Nakajima, Y. Honda, O. Kitao, H. Nakai, M. Klene, X. Li, J. E. Knox, H. P. Hratchian, J. B. Cross, V. Bakken, C. Adamo, J. Jaramillo, R. Gomperts, R. E. Stratmann, O. Yazyev, A. J. Austin, R. Cammi, C. Pomelli, J. W. Ochterski, P. Y. Ayala, K. Morokuma, G. A. Voth, P. Salvador, J. J. Dannenberg, V. G. Zakrzewski, S. Dapprich, A. D. Daniels, M. C. Strain, O. Farkas, D. K. Malick, A. D. Rabuck, K. Raghavachari, J. B. Foresman, J. V. Ortiz, Q. Cui, A. G. Baboul, S. Clifford, J. Cioslowski, B. B. Stefanov, G. Liu, A. Liashenko, P. Piskorz, I. Komaromi, R. L. Martin, D. J. Fox, T. Keith, M. A. Al-Laham, C. Y. Peng, A. Nanayakkara, M. Challacombe, P. M. W. Gill, B. Johnson, W. Chen, M. W. Wong, C. Gonzalez, and J. A. Pople, *Gaussian 03, Revision C.02*. Gaussian, Inc., Wallingford, CT, 2004.

[10] S. Goedecker and G. E. Scuseria, *Linear scaling electronic structure methods in chemistry and physics*, Computing in Science and Engineering, 5 (2003), pp. 14–21.

[11] L. Greengard, *The rapid evaluation of potential fields in particle systems*, MIT Press, 1987.

[12] M. F. Guest, E. Apra, D. E. Bernholdt, R. J. Harrison, R. A. Kendall, and R. A. Kutteh, *High performance computational chemistry: Nwchem and fully distributed parallel applications*, in Applied Parallel Computing - Computations in Physics, Chemistry and Engineering Science, J. Dongarra, K. Madsen, and J. Wasniewski, eds., Springer, Berlin,, 1996, pp. 278–294.

[13] O. Gunnarsson and R. O. Jones, *Density functional calculations for atoms, molecules and clusters*, Phys. Scr., 21 (1980).

[14] P. Hohenberg and W. Kohn, *Inhomogenous electron gas*, Phys. Rev., **136** (1964), pp. B864–B871.

[15] F. Jensen, *Introduction to Computational Chemistry*, John Wiley & Sons Inc., New York, 1998.

[16] J. Knap and M. Ortiz, *An analysis of the quasicontinuum method*, Journal of the Mechanics and Physics of Solids, 49 (2001), pp. 1899–1923.

[17] W. Koch and M. C. Holthausen, *A Chemist's Guide to Density Functional Theory*, John Wiley & Sons Inc., New York, second ed., 2001.

[18] W. Kohn and L. J. Sham, *Self-consistent equations including exchange and correlation effects*, Phys. Rev., **140** (1965), pp. A1133–A1138.

[19] R. E. Miller and E. B. Tadmor, *The quasicontinuum method: Overview, applications and current directions*, Journal of Computer-Aided Materials Design, 9 (2002), pp. 203–239.

[20] R. G. Parr and W. Yang, *Density-Functional Theory of Atoms and Molecules*, Oxford University Press, Oxford, 1994.

[21] M. Payne, M. Teter, D. Allan, T. Arias, and J. Joannopoulos, *Iterative minimization techniques for ab initio total-energy calculations: molecular dynamics and conjugate gradients*, Rev.Mod.Phys., 64 (1992), pp. 1045–1097.

[22] J. P. Perdew and Y. Wang, *Accurate and simple analytic representation of the electron-gas correlation-energy*, Phys. Rev., **B45** (1992), p. 13244.

[23] J. P. Perdew and A. Zunger, *Self-interaction correction to Density Functional approximations for many-electron systems*, Phys. Rev., **B23** (1981), pp. 5048–5079.

[24] H. G. Petersen, D. Soelvason, J. W. Perram, and E. R. Smith, *The very fast multipole method*, J. Chem. Phys., 101 (1994), pp. 8870–8876.

[25] C.-K. Skylaris, P. D. Haynes, A. A. Mostofi, and M. C. Payne, *Introducing ONETEP: Linear-scaling density functional simulations on parallel computers*, The Journal of Chemical Physics, 122 (2005), p. 084119.

[26] E. Tadmor, M. Ortiz, and R. Phillips, *Quasicontinuum analysis of defects in solids*, Philosophical Magazine A, 73 (1996), pp. 1529–1563.

[27] L. H. Thomas, *The calculation of atomic fields*, Proc. Camb. Phil. Soc., **23** (1927), pp. 542–548.

[28] O. Treutler and R. Ahlrichs, *Efficient molecular numerical integration schemes*, The Journal of Chemical Physics, 102 (1995), pp. 346–354.

[29] L.-W. Wang and E. A. Carter, *Orbital-free kinetic-energy density functional theory*, in Theoretical methods in condensed phase chemistry Progress in Theoretical Chemistry and Physics, S. D. Schwartz, ed., Kluwer, Dordrecht, 2000, pp. 117–184.

Appendix

A The Domain Decomposition Approach for Thomas-Fermi DFT

Within the Born-Oppenheimer framework, the electronic density minimizes the energy functional $E[\rho, \{\mathbf{R}_A\}]$ of Eq.(7), subject to the charge conservation constraint of Eq.(2b). If $\rho(\mathbf{r})$ is optimal, $\delta E[\rho; \{\mathbf{R}_A\}] = 0$ for any change $\delta\rho(\mathbf{r})$ that is consistent with the charge constraint, in other words, that satisfies

$$\int \delta\rho \mathrm{d}\mathbf{r} = 0 \,. \tag{53a}$$

If one suitably defines

$$\mathcal{F}[\rho(\mathbf{r}); \{\mathbf{R}_A\}] = \frac{5}{3} C_F \rho^{\frac{2}{3}}(\mathbf{r}) - \frac{4}{3} C_x \rho^{\frac{1}{3}}(\mathbf{r}) + \int_D \frac{\rho(\mathbf{r}')}{||\mathbf{r} - \mathbf{r}'||} \mathrm{d}\mathbf{r}' - \sum_{A=1}^{M} \frac{Z_A}{||\mathbf{r} - \mathbf{R}_A||} \,, \tag{53b}$$

the condition

$$\delta E[\rho, \{\mathbf{R}_A\}] = \int_D \mathcal{F}[\rho(\mathbf{r}); \{\mathbf{R}_A\}] \, \delta\rho(\mathbf{r}) \mathrm{d}\mathbf{r} = 0 \tag{53c}$$

should hold for any variation $\delta\rho(\mathbf{r})$ that satisfies the condition of Eq.(53a). Consequently, $\mathcal{F}[\rho(\mathbf{r}); \{\mathbf{R}_A\}]$ is constant, and by convention this constant is denoted by λ. Thus, an optimal $\rho(\mathbf{r})$ must necessarily satisfy

$$\mathcal{F}[\rho(\mathbf{r}); \{\mathbf{R}_A\}] + \lambda = 0 \tag{54a}$$

$$\int_D \rho(\mathbf{r}) \mathrm{d}\mathbf{r} - N_e = 0 \tag{54b}$$

Next, consider that the domain D is partitioned in two disjoint subdomains $D_1 \cup D_2 = D$, in order to prove that by appropriately defining the external potential in each of these two subdomains, and then solving the associated electronic problem in each domain, will produce the same solution $\rho(\mathbf{r})$ that the problem in Eq.(54) leads to. For this to happen, the following two conditions must be satisfied:

1. When solving the electronic structure problem in D_1, the density ρ_2 in the domain D_2 is considered fixed; in other words, the energy functional E^1 associated with D_1 depends parametrically on ρ_2:

$$\begin{aligned} E^1[\rho_1; \bar{\rho}_2, \{\mathbf{R}_A\}] = {} & C_F \int_{D_1} \rho_1^{\frac{5}{3}}(\mathbf{r}) \, \mathrm{d}\mathbf{r} - C_x \int_{D_1} \rho_1^{\frac{4}{3}}(\mathbf{r}) \, \mathrm{d}\mathbf{r} + \frac{1}{2} \int_{D_1} \int_{D_1} \frac{\rho_1(\mathbf{r}) \, \rho_1(\mathbf{r}')}{\|\mathbf{r} - \mathbf{r}'\|} \, \mathrm{d}\mathbf{r} \, \mathrm{d}\mathbf{r}' \\ & + \int_{D_1} \int_{D_2} \frac{\rho_1(\mathbf{r}) \, \bar{\rho}_2(\mathbf{r}')}{\|\mathbf{r} - \mathbf{r}'\|} \, \mathrm{d}\mathbf{r}' \, \mathrm{d}\mathbf{r} - \sum_{A=1}^{M} Z_A \int_{D_1} \frac{\rho_1(\mathbf{r})}{\|\mathbf{r} - \mathbf{R}_A\|} \, \mathrm{d}\mathbf{r} \end{aligned} \tag{55a}$$

   Note the introduction of the cross-domain interaction term

$$\int_{D_1} \int_{D_2} \frac{\rho_1(\mathbf{r}) \, \bar{\rho}_2(\mathbf{r}')}{\|\mathbf{r} - \mathbf{r}'\|} \, \mathrm{d}\mathbf{r}' \, \mathrm{d}\mathbf{r} \,,$$

2. When solving the electronic structure problem in D_2, the density ρ_1 in the domain D_1 is considered fixed; in other words, the energy functional E^2 associated with D_2 depends parametrically on ρ_1:

$$\begin{aligned} E^2[\rho_2; \bar{\rho}_1, \{\mathbf{R}_A\}] = {} & C_F \int_{D_2} \rho_2^{\frac{5}{3}}(\mathbf{r}) \, \mathrm{d}\mathbf{r} - C_x \int_{D_2} \rho_2^{\frac{4}{3}}(\mathbf{r}) \, \mathrm{d}\mathbf{r} + \frac{1}{2} \int_{D_2} \int_{D_2} \frac{\rho_2(\mathbf{r}) \, \rho_2(\mathbf{r}')}{\|\mathbf{r} - \mathbf{r}'\|} \, \mathrm{d}\mathbf{r} \, \mathrm{d}\mathbf{r}' \\ & + \int_{D_2} \int_{D_1} \frac{\rho_2(\mathbf{r}) \, \bar{\rho}_1(\mathbf{r}')}{\|\mathbf{r} - \mathbf{r}'\|} \, \mathrm{d}\mathbf{r}' \, \mathrm{d}\mathbf{r} - \sum_{A=1}^{M} Z_A \int_{D_2} \frac{\rho_1(\mathbf{r})}{\|\mathbf{r} - \mathbf{R}_A\|} \, \mathrm{d}\mathbf{r} \end{aligned} \tag{55b}$$

   Note the introduction of the cross-domain interaction term

$$\int_{D_2} \int_{D_1} \frac{\rho_2(\mathbf{r}) \, \bar{\rho}_1(\mathbf{r}')}{\|\mathbf{r} - \mathbf{r}'\|} \, \mathrm{d}\mathbf{r}' \, \mathrm{d}\mathbf{r} \,.$$

3. The charge conservation constraints assumes the form

$$\int_{D_1} \rho_1(\mathbf{r})\, \mathrm{d}\mathbf{r} + \int_{D_2} \rho_2(\mathbf{r})\, \mathrm{d}\mathbf{r} - N_e = 0\,. \tag{55c}$$

The electronic problems are solved independently in D_1 and D_2, the coupling coming through Eq.(55c). The solution process starts with initial guesses for $\rho_1(\mathbf{r})$ and $\rho_2(\mathbf{r})$ and repeatedly solves the electronic problems in D_1 and D_2 until the change in $\rho_1(\mathbf{r})$ and $\rho_2(\mathbf{r})$ between successive iterations becomes negligible.

In this framework, the first order optimality conditions for the electronic problems in D_1 and D_2; i.e.,

$$\delta E_1\left[\rho_1; \bar{\rho}_2, \{\mathbf{R}_A\}\right] = 0 \tag{56a}$$

$$\delta E^2\left[\rho_2; \bar{\rho}_1, \{\mathbf{R}_A\}\right] = 0\,, \tag{56b}$$

should hold for any set of changes in density $\delta\rho_1(\mathbf{r})$ and $\delta\rho_2(\mathbf{r})$ that satisfy

$$\int_{D_1} \delta\rho_1(\mathbf{r})\, \mathrm{d}\mathbf{r} + \int_{D_2} \delta\rho_1(\mathbf{r})\, \mathrm{d}\mathbf{r} = 0\,. \tag{56c}$$

For $\mathbf{r} \in D_1$, by suitably defining

$$\mathcal{F}^1\left[\rho_1(\mathbf{r}); \bar{\rho}_2(\mathbf{r}), \{\mathbf{R}_A\}\right] = \frac{5}{3}C_F\rho_1^{\frac{2}{3}}(\mathbf{r}) - \frac{4}{3}C_x\rho_1^{\frac{1}{3}}(\mathbf{r}) + \int_{D_1} \frac{\rho_1(\mathbf{r}')}{||\mathbf{r}-\mathbf{r}'||}\mathrm{d}\mathbf{r}' + \int_{D_2} \frac{\bar{\rho}_2(\mathbf{r}')}{||\mathbf{r}-\mathbf{r}'||}\mathrm{d}\mathbf{r}' - \sum_{A=1}^{M} \frac{Z_A}{||\mathbf{r}-\mathbf{R}_A||} \tag{57a}$$

and, for $\mathbf{r} \in D_2$, defining

$$\mathcal{F}^2\left[\rho_2(\mathbf{r}); \bar{\rho}_1(\mathbf{r}), \{\mathbf{R}_A\}\right] = \frac{5}{3}C_F\rho_2^{\frac{2}{3}}(\mathbf{r}) - \frac{4}{3}C_x\rho_2^{\frac{1}{3}}(\mathbf{r}) + \int_{D_1} \frac{\bar{\rho}_1(\mathbf{r}')}{||\mathbf{r}-\mathbf{r}'||}\mathrm{d}\mathbf{r}' + \int_{D_2} \frac{\rho_2(\mathbf{r}')}{||\mathbf{r}-\mathbf{r}'||}\mathrm{d}\mathbf{r}' - \sum_{A=1}^{M} \frac{Z_A}{||\mathbf{r}-\mathbf{R}_A||} \tag{57b}$$

the first-order optimality conditions become

$$\int_{D_1} \mathcal{F}^1\left[\rho_1(\mathbf{r}); \bar{\rho}_2(\mathbf{r}), \{\mathbf{R}_A\}\right] \delta\rho_1(\mathbf{r}) = 0 \tag{58a}$$

$$\int_{D_2} \mathcal{F}^2\left[\rho_2(\mathbf{r}); \bar{\rho}_1(\mathbf{r}), \{\mathbf{R}_A\}\right] \delta\rho_2(\mathbf{r}) = 0\,, \tag{58b}$$

which must hold for any perturbations $\delta\rho_1(\mathbf{r})$ and $\delta\rho_2(\mathbf{r})$ that satisfy Eq.(56c). Then there should be a constant μ such that $\rho_1(\mathbf{r})$, $\rho_2(\mathbf{r})$, and μ are the solution of the integral system

$$\begin{aligned}
\mathcal{F}^1\left[\rho_1(\mathbf{r}); \bar{\rho}_2(\mathbf{r}), \{\mathbf{R}_A\}\right] + \mu &= 0 && (59a)\\
\mathcal{F}^2\left[\rho_2(\mathbf{r}); \bar{\rho}_1(\mathbf{r}), \{\mathbf{R}_A\}\right] + \mu &= 0 && (59b)\\
\int_{D_1} \rho_1(\mathbf{r})\mathrm{d}\mathbf{r} + \int_{D_2} \rho_2(\mathbf{r})\mathrm{d}\mathbf{r} - N_e &= 0\,. && (59c)
\end{aligned}$$

In what follows, denote by $\tilde{\rho}_1(\mathbf{r})$ and $\tilde{\rho}_2(\mathbf{r})$ the solution of the above system, and define

$$\rho(\mathbf{r}) = \begin{cases} \tilde{\rho}_1(\mathbf{r}) & \mathbf{r} \in D_1 \\ \tilde{\rho}_2(\mathbf{r}) & \mathbf{r} \in D_2 \end{cases}$$

For any $\mathbf{r} \in D$, either $\mathbf{r} \in D_1$, or $\mathbf{r} \in D_2$. From Eq.(59a) in the first case, or Eq.(59b) in the second case, $\tilde{\rho}(\mathbf{r})$ must satisfy

$$\begin{aligned}
\frac{5}{3}C_F\tilde{\rho}^{\frac{2}{3}}(\mathbf{r}) - \frac{4}{3}C_x\tilde{\rho}^{\frac{1}{3}}(\mathbf{r}) + \int_{D} \frac{\tilde{\rho}(\mathbf{r}')}{||\mathbf{r}-\mathbf{r}'||}\mathrm{d}\mathbf{r}' - \sum_{A=1}^{M} \frac{Z_A}{||\mathbf{r}-\mathbf{R}_A||} + \mu &= 0 && (60a)\\
\int_{D} \tilde{\rho}(\mathbf{r})\mathrm{d}\mathbf{r} - N_e &= 0\,. && (60b)
\end{aligned}$$

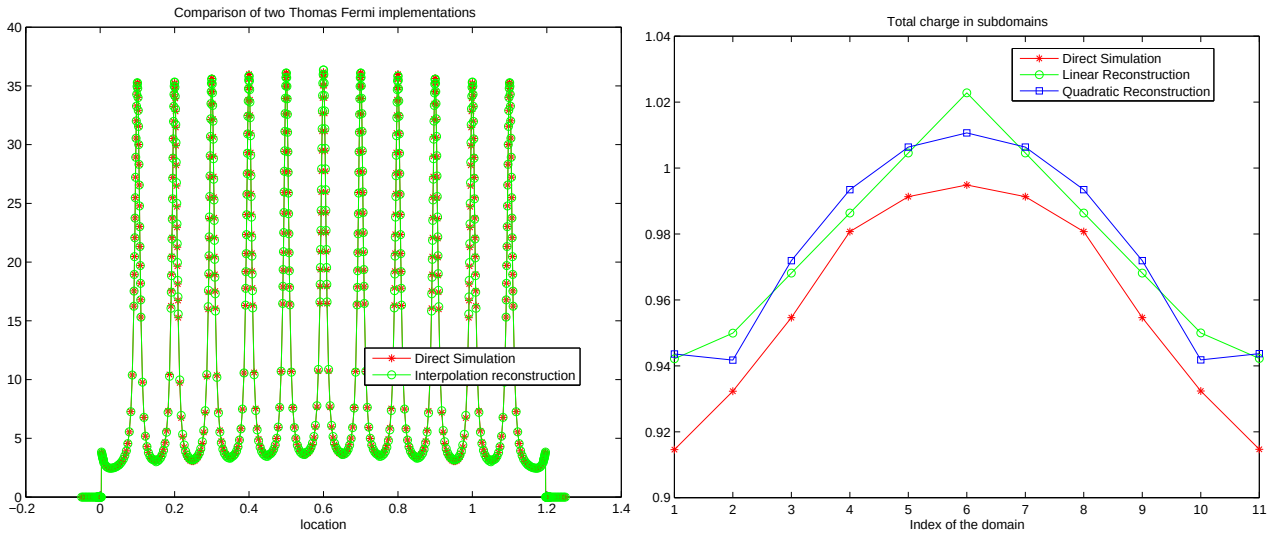

Figure 5: Solutions and Total Charge resulting from direct minimization of the Thomas Fermi functional and from the minimization of the Thomas Fermi functional with density reconstruction

This is, however, precisely the problem that provides the solution $\rho(\mathbf{r})$ for the original problem, defined over the whole domain D (see Eq.(54)). Therefore, $\rho(\mathbf{r}) = \tilde{\rho}(\mathbf{r})$ and $\lambda = \mu$.

Conversely, suppose that $\rho(\mathbf{r})$ and λ are such that the conditions of Eq.(54) hold for any $\mathbf{r} \in D$. Define $\rho_1(\mathbf{r}) = \rho(\mathbf{r})$ for any $\mathbf{r} \in D_1$, and $\rho_2(\mathbf{r}) = \rho(\mathbf{r})$ for any $\mathbf{r} \in D_2$; that is, define $\rho_1(\mathbf{r})$ and $\rho_2(\mathbf{r})$ to be the restrictions of $\rho(\mathbf{r})$ to D_1 and D_2, respectively. Writing Eq.(54a) for any $\mathbf{r} \in D_1$ indicates that Eq.(59a) holds, while writing Eq.(54a) for $\mathbf{r} \in D_2$ suggests that Eq.(59b) holds. Since $D = D_1 \cup D_2$, the charge conservation condition in Eq.(54b) can be expressed as in Eq.(59c). In other words, the solution of the electronic problem in D provides for the solution of the electronic problem in the subdomains.

To conclude, one can divide the large problem and solve smaller electronic problems on the subdomains, with the caveat that the potential (the cross-domain interaction) should be appropriately defined as indicated earlier. Conversely, the electronic density in the big domain provides for the solution of the electronic density problem in each subdomain.

Finally, the assumption that D was partitioned in two subdomains D_1 and D_2 was introduced to keep the presentation simple. The same argument holds if D is partitioned in more subdomains, and the electronic problem is solved in each of these domains in parallel with appropriately defined cross-domain potentials..

B Numerical Results

In this section, we compare the numerical results from the direct minimization approach of the Thomas Fermi functional with the ones from the procedure described in Subsection (3.2).

Out one-dimensional setup is very similar to the one in Figure (2). We take 11 equally spaced nuclei with unit charge, $Z_A = 1$, and we take the total number of electrons N to be equal to 11. The location of the atoms coresponds to the peaks seen in Figure (5). We construct a mesh that has 50 nodes per cell, with 30 of them equally spaced on an interval centered at the position of the atom and whose length is 1/5 of the distance between two atoms. We therefore have 11 domains, D_1, D_2, ..., D_{11}. For discretization of the integral operators we use the trapezoidal rule. When doing interpolation, we use only the domains D_2, D_6,D_{10} in order to avoid the boundary distortion. We use either piecewise linear or quadratic interpolations for the interpolation-based approach. We chose the parameter $\delta = 10^{-4}$, with a slightly different regularization than described in the previous sections whereby terms of the type $1/||\cdot||$ are replaced with $1/||\cdot + \delta||$.

We solve the resulting electronic structure optimization problem with the augmented Lagrangian software Lancelot [6], which uses an iterative method to solve the bound constrained subproblem, that is obtained after penalization of the constraints. When using the interpolation method, we enforce the interpolation conditions (26) as constraints, rather than substituting them in the functional that describes the problem (43). In an actual large scale implementation, the substitution would be carried out, and only the electronic density degrees of

freedom in D_1, D_2,D_6,D_{10},D_{11} will be considered. In this work, we are seeking to evaluate the potential of interpolation-based reconstruction without regard to computational efficiency, at the moment.

The solution of the direct numerical simulation and of the linear-interpolation-based optimization are depicted in Figure 5. We can see that they are indistinguishable, which means that the interpolation approach was highly succesfull at reconstructing the solution in the "gap" domains. The same is true for the quadratic-interpolation-based reconstruction which is not depicted since the ticker overlap would reduce the quality of the figure. Note, however, that the solutions are not identical. This can be seen by computing the total charge in the subdomains. The results for the three methods are presented in Figure 5, the right panel. We see that the quadratic interpolation method produced a very good fit, with a relative error that is uniformly bellow 2% for domains 2 to 10. Note that a periodic approach (which is equivalent to requesting that all domains from D_2 to D_{10} have the same density must result in an error of the total charge that must exceed 4% for some subdomains.

The solution presents some irregular artifacts at the very end of the domain. That in itself is not that surprising, given that the Thomas-Fermi theory is asymptotically valid in the bulk. We want to stress that we do not investigate here how good of a prediction a DFT such as Thomas Fermi can make; rather we are investigating the potential of density reconstruction methods to reduce computational effort while retaining high accuracy and moving beyond periodic boundary conditions, which, from our computations and theoretical developments, seems to be very high.

In future work, we will investigate the extension of these conclusions to other DFT approaches.